VU VRIJE UNIVERSITEIT AMSTERDAM

VU Research Portal

Bifurcations at infinity in a model for 1:4 resonance.

Krauskopf, B.

published in
Ergodic theory and dynamical systems
1997

DOI (link to publisher)
10.1017/S0143385797085039

document version
Publisher's PDF, also known as Version of record

Link to publication in VU Research Portal

citation for published version (APA)
Krauskopf, B. (1997). Bifurcations at infinity in a model for 1:4 resonance. *Ergodic theory and dynamical systems*, *17*(4), 899-931. https://doi.org/10.1017/S0143385797085039

General rights
Copyright and moral rights for the publications made accessible in the public portal are retained by the authors and/or other copyright owners and it is a condition of accessing publications that users recognise and abide by the legal requirements associated with these rights.

- Users may download and print one copy of any publication from the public portal for the purpose of private study or research.
- You may not further distribute the material or use it for any profit-making activity or commercial gain
- You may freely distribute the URL identifying the publication in the public portal ?

Take down policy
If you believe that this document breaches copyright please contact us providing details, and we will remove access to the work immediately and investigate your claim.

E-mail address:
vuresearchportal.ub@vu.nl

Download date: 04. May. 2023

Ergod. Th. & Dynam. Sys. (1997), **17**, 899–931
Printed in the United Kingdom © *1997 Cambridge University Press*

Bifurcations at ∞ in a model for 1:4 resonance

BERND KRAUSKOPF†
Vakgroep Wiskunde, Rijksuniversiteit Groningen, 9700 AV Groningen, The Netherlands

(*Received* 13 *April* 1995 *and revised* 11 *May* 1996)

Abstract. The equation $\dot{z} = e^{i\alpha}z + e^{i\varphi}z|z|^2 + b\bar{z}^3$ models a map near a Hopf bifurcation with 1:4 resonance. It is a conjecture by V. I. Arnol'd that this equation contains all versal unfoldings of $\mathbb{Z}_4$-equivariant planar vector fields. We study its bifurcations at ∞ and show that the singularities of codimension two unfold versally in a neighborhood. We give an unfolding of the codimension-three singularity for $b = 1$, $\varphi = 3\pi/2$ and $\alpha = 0$ in the system parameters and use numerical methods to study global phenomena to complete the description of the behavior near ∞. Our results are evidence in support of the conjecture.

1. *Introduction*

The 1:4 resonance problem can very briefly be introduced as follows; see [**Kra95**] for a detailed introduction. The Poincaré map of a closed orbit near 1:q resonance can be approximated up to any prescribed order by the time-one map of a $\mathbb{Z}_q$-equivariant planar vector field composed with the rotation by $2\pi/q$. Today all versal unfoldings of $\mathbb{Z}_q$-equivariant planar vector fields for $q \neq 4$ are known, which provides an answer for all resonances except for the case of 1:4 resonance; see [**Arn77**, **Arn78**, **AAIS86**, **Bog76a**, **Bog76b**, **Ca81**, **Kho79**, **Ta74b**].

We are concerned with the remaining problem of finding all unfoldings of $\mathbb{Z}_4$-equivariant planar vector fields. Any such vector field can be written as

$$\dot{z} = \epsilon z + Az|z|^2 + B\bar{z}^3 + O(|z|^5),$$

where ϵ, A, $B \in \mathbb{C}$. This gave rise to a classical conjecture.

CONJECTURE 1. (Arnol'd 1977) *In the class of $\mathbb{Z}_4$-equivariant planar vector fields, the* principal part

$$\dot{z} = \varepsilon z + Az|z|^2 + B\bar{z}^3 \tag{1}$$

contains all versal unfoldings in the parameter $\varepsilon \in \mathbb{C}$ of the singularity $\varepsilon = 0$, depending on A, $B \in \mathbb{C}$.

† Current address: Theoretische Natuurkunde, Vrije Universiteit, 1081 HV Amsterdam, The Netherlands (email: berndk@nat.vu.nl).

- *There are finitely many submanifolds of codimension one in* (A, B)*-space where (A,B) is non-generic, by which it is meant that (1) is not a versal unfolding.*
- *These manifolds divide* (A, B)*-space in finitely many open and connected regions on which (1) is a versal unfolding.*
- *Unfoldings for* (A, B) *from the same region are topologically equivalent.*

Remark 2. As part of this conjecture Arnol'd has given a list of genericity conditions on (A, B) and of unfoldings in open regions of (A, B)-space.

In order to prove this conjecture one has to know all equivalence classes of unfoldings of (1) for generic nonlinear terms given by (A, B). In a second step one then has to show some robustness of these unfoldings in the sense that a perturbation by higher-order terms does not change them essentially. Note that the difficulty in this case comes from the fact that the two nonlinear terms are of the same order.

Scaling phase space and time clearly does not change the equivalence class of an unfolding. This can be used to reduce (1) to

$$\dot{z} = e^{i\alpha} z + e^{i\varphi} z|z|^2 + b\bar{z}^3, \tag{2}$$

where $\alpha \in (-\pi, \pi]$, $\varphi \in [\pi, \frac{3}{2}\pi]$ and $b \in \mathbb{R}^+$. Due to the reduction we lost the central singularity for $\varepsilon = 0$. The dimension of the parameter space has become smaller but the codimensions of the bifurcations remain the same; see [**Kra94b**, **Kra95**] for more details.

In what follows we study (2) and regard b, φ and α as parameters on equal terms. The bifurcation set dividing (b, φ, α)-space into regions of equivalent phase portraits has been studied in [**Kra94b**] and is shown in Figure 1. It consists of surfaces of codimension-one bifurcations, which typically meet in curves of codimension-two bifurcations. The information about the unfoldings of (1) can be obtained by collecting all phase portraits that are encountered under the variation of α, a procedure we call *drilling*. The problem of finding all unfoldings has been translated to finding all surfaces in the bifurcation set. In [**Kra94b**] the reader can find arguments why the presented model of the bifurcation set is correct and complete. Here we study the open problem of what happens along the line $b = 1$, $\varphi = 3\pi/2$, $\alpha \in (-\pi, \pi]$. This turns out to be the study of bifurcations at ∞. In particular, we are interested in the point $b = 1$, $\varphi = 3\pi/2$, $\alpha = 0$; see Figure 1.

Due to the scalings used to obtain (2), the whole phase space $\mathbb{C}$ is important. Hence, we have to take into account what happens at ∞. If a limit cycle or an equilibrium escapes to ∞, this must be considered a bifurcation. Blowing up the point ∞ in (2) gives

$$\dot{r} = -(\cos\varphi + b\sin\theta)r - \cos\alpha\, r^3, \quad \dot{\theta} = 4(\sin\varphi + b\cos\theta) + 4\sin\alpha\, r^2, \tag{3}$$

a reflectionally equivariant vector field on the cylinder $\mathbb{R} \times \mathbb{R}/2\pi\mathbb{Z}$ with the invariant circle $\{r = 0\}$. The symmetry group is generated by the reflection $(r, \theta) \mapsto (-r, \theta)$. In this paper we study the bifurcations on the invariant circle of (3), corresponding to bifurcations at ∞ of (2).

Results.

(a) For $b = 1$, $\varphi = 3\pi/2$ and $\alpha \notin \{0, \pm\pi/2, \pi\}$ there are two types of codimension-two singularities on the invariant circle $\{r = 0\}$. They unfold versally in a neighborhood with the parameters b and φ.

(b) For $b = 1$, $\varphi = 3\pi/2$ and $\alpha = 0$ there is a singularity of at least codimension three on the invariant circle $\{r = 0\}$. We give an unfolding in a neighborhood with the parameters b, φ and α.

(c) The point in parameter space $b = 1$, $\varphi = 3\pi/2$ and $\alpha = 0$ is an organizing center of (2): arbitrarily close to it, all equivalence types of phase portraits can be found. By combining (b) with numerical results we obtain the global picture in a neighborhood of the organizing center.

(d) The model of the bifurcation set presented in [**Kra94b**] is confirmed by the above results and by computing global bifurcation surfaces close to $b = 1$, $\varphi = 3\pi/2$ for fixed α. This is support for Conjecture 1.

Known results from the literature about reflectionally equivariant planar vector fields can be used to show (a). The proof of (b) essentially consists of finding the unfolding of the corresponding codimension-three singularity in the class of reflectionally equivariant planar vector fields, which is joint work with Rousseau; see [**KR96**]. With numerical techniques we get the global picture in a neighborhood of the organizing center to obtain (c). Combining all results confirms our model of the bifurcation set, which constitutes a step towards proving Conjecture 1. We did not find as yet unknown bifurcations of (2) or, equivalently, as yet unknown unfoldings. There is hope that the method of desingularizing a family, presented in [**Du93**, **Rou93a**, **Rou93b**, **Pan97**], may lead to further progress in the still missing analytical study of the global phenomena.

This paper is organized as follows. In §2 we briefly present the bifurcation set. §3 explains why the bifurcations at ∞ of (2) are important. This is illustrated with the example of the Hopf bifurcation in §4. The blow-up procedure leading to (3) is the topic of §5. In §6 we discuss the codimension-one bifurcations and then turn to the singularities on the invariant circle for $b = 1$, $\varphi = 3\pi/2$ in §7. The two cases of codimension-two singularities, called case '$-$' and case '$+$', are studied in §8. The singularity for $b = 1$, $\varphi = 3\pi/2$, $\alpha = 0$, giving the connection between case '$-$' and case '$+$', is studied in §9. Global phenomena due to the geometry of the cylinder are discussed in §10.

2. *Background*

In the classical formulation of Conjecture 1, there is a clear distinction between the unfolding *parameter* α and the *constants* (b, φ) which determine the nonlinear terms. Given (b, φ), the collection of all topologically different phase portraits, as α is continuously varied from $-\pi$ to π, is called a *bifurcation sequence*. Two *bifurcation sequences are topologically equivalent* if the bifurcations occur in the same order and the respective phase portraits are topologically equivalent. In the study of (2) the notion of topological equivalence of unfoldings translates to the topological equivalence of bifurcation sequences.

The question is how the (b, φ)-plane is divided into regions of topologically equivalent bifurcation sequences. The (b, φ)-plane is shown in Figure 2 and the reader is referred

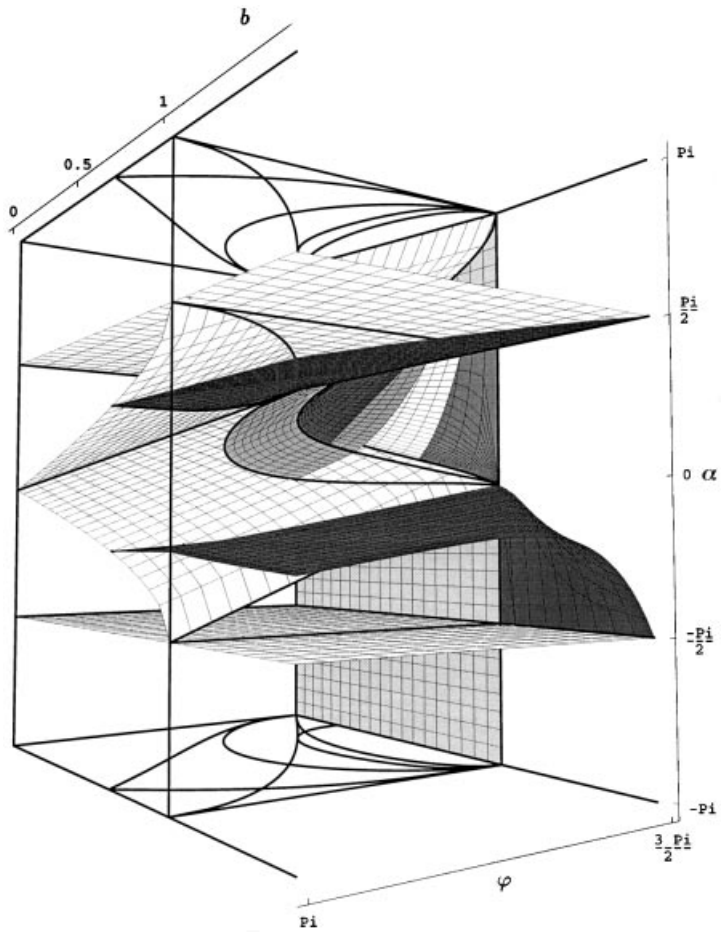

FIGURE 1. The bifurcation set for $\varphi \in [\pi, 3\pi/2]$ and $0 \leq b \leq 1.5$. Some of the surfaces have been cut open so that all surfaces can be seen. Also included is the surface $\odot^{\infty}$ of Hopf bifurcations at ∞, given by $\varphi = 3\pi/2$, $b \in [0, 1]$. Note that the surface $\pitchfork^{\infty}$ of pitch-fork bifurcations at ∞, given by $b = 1$, is not shown. See Figure 3 and Table 1 for an explanation of the surfaces and curves.

to [**BK79**, **CLW94**, **Kra94a**, **Kra95**] for an inventory of all known bifurcation sequences. Note that the (b, φ)-plane is a transformation of the 'A-plane' which can be found in the classical literature and compare [**Kra94b**] for the connection between the two.

It turns out to be useful to disregard the distinction between the parameter α and the constants (b, φ). We consider b, φ and α as parameters on equal terms of the vector field (2) with the three-dimensional parameter (b, φ, α)-space. (This is not to be mixed up with the fact that the original task is to find all versal two-parameter unfoldings in the space of $\mathbb{Z}_4$-equivariant planar vector fields.) It is in the spirit of bifurcation theory to ask how (b, φ, α)-space is divided into regions of topologically different phase portraits. In other words, we ask for the equivalence classes under the simpler notion of topological equivalence of just phase portraits.

This leads to the study of the bifurcation set dividing (b, φ, α)-space into regions of equivalent phase portraits; for details and color figures see [**Kra94b**]. The bifurcation set is shown in Figure 1 as a three-dimensional Mathematica plot (see [**Wo88**]), while Figure 3 consists of two cross-sections with the labeling of the surfaces and open regions of phase portraits. For reference, the symbols of the surfaces and curves in the bifurcation set are listed in Table 1.

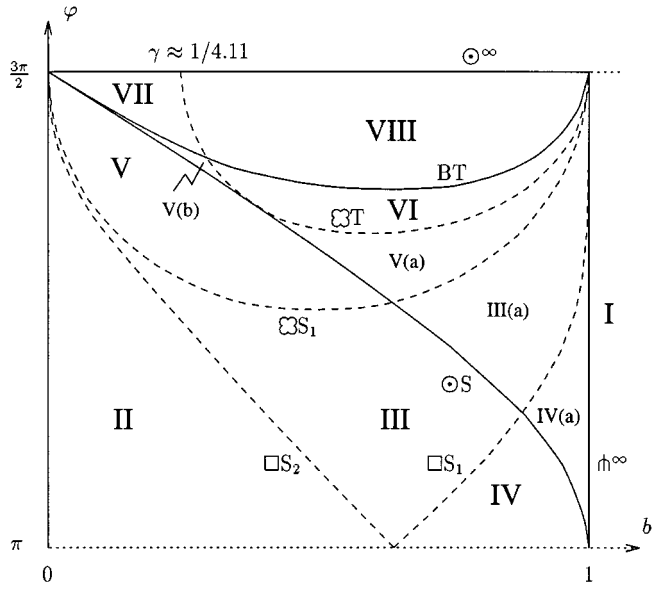

FIGURE 2. The (b, φ)-plane of (2) showing the regions of different bifurcation sequences, which can be found in [**Kr94a**]. The solid curves are known analytically; the dashed ones are not, but are adapted from [**BK79**, **BK80**]. For the curve labels see Table 1.

The bifurcation sequence for given (b, φ) can be found by drilling in the direction of α, that is, by collecting all phase portraits that are encountered under the variation of α. Consequently, in order to find all versal unfoldings of (1) we need to find all surfaces in the bifurcations set of (2). In this paper we continue the work in [**Kra94b**] of showing that our model of the bifurcation set is correct by studying the bifurcations at ∞ of (2).

The boundary lines $\odot^\infty$ and $\pitchfork^\infty$ in the (b, φ)-plane correspond to Hopf and pitchfork bifurcations at ∞; see Figure 2. Looking at Figure 1 it becomes clear that the line $b = 1$, $\varphi = 3\pi/2$, $\alpha \in (-\pi, \pi]$ plays a special role: the surfaces T_+, $\dagger$, $\heartsuit$, $\circledcirc$ and $\square_1$ accumulate on it, which means that these surfaces cannot be parametrized by their values of α over the (b, φ)-plane above the point $b = 1$, $\varphi = 3\pi/2$. (Note that everywhere else this is possible.) It turns out that for $b = 1$, $\varphi = 3\pi/2$, there are singularities at ∞ of codimension at least two, the type of which depends on the value of α. The bifurcations at ∞ organize the neighborhood of the line $b = 1$, $\varphi = 3\pi/2$, $\alpha \in (-\pi, \pi]$, much like the classical example of such a phenomenon, the lines $\varphi = 3\pi/2$ and $\alpha = \pm\pi/2$, where the system is Hamiltonian; see [**Nei78**]. The knowledge of what can bifurcate from the different Hamiltonian cases played an important role in completing the list of known

Surface	Characterizing property	
$\odot_1$	First Hopf bifurcation at 0	L
$\odot_2$	Second Hopf bifurcation at 0	L
S_1	First saddle-node bifurcation	L
S_2	Second saddle-node bifurcation	L
T_-	Trace is zero at the saddles	L
T_+	Trace is zero at the nodes (Hopf bifurcation at secondary equilibria)	L
$\pitchfork^\infty$	Pitchfork bifurcation at ∞	L
S^∞	Saddle-node bifurcation at ∞	L
$\odot^\infty$	Hopf bifurcation at ∞	NL
$\dashv$	Homoclinic loop at secondary equilibria	NL
$\square_1$	First square connection	NL
$\square_2$	Second square connection	NL
$\clubsuit$	Clover connection	NL
$\circledcirc$	Saddle-node of limit cycles	NL

Curve	Characterizing property	
$\odot$S	Hopf bifurcation at 0 coincides with second saddle-node bifurcation	L
BT	Bogdanov–Takens bifurcation	L
$\clubsuit$T	Clover connection with zero trace	NL
$\clubsuit S_1$	Clover connection coincides with first saddle-node bifurcation	NL
$\square S_1$	Square connection coincides with first saddle-node bifurcation	NL
$\square S_2$	Square connection coincides with second saddle-node bifurcation	NL

TABLE 1. Symbols for surfaces of codimension-one bifurcations and curves of codimension-two bifurcations. The last column indicates whether the surface or curve comes from a local bifurcation or not. The surfaces $\odot^\infty$ and $\pitchfork^\infty$ lead to boundary curves in the (b, φ)-plane, for which we use the same symbols, the surface S^∞ does not.

bifurcation sequences.

The point $b = 1$, $\varphi = 3\pi/2$, $\alpha = 0$ is of special interest. We call it an organizing center, since in an arbitrary neighborhood of this point one can find all equivalence types of phase portraits. We give a description of the corresponding singularity at ∞ and an unfolding in a neighborhood in the system parameters.

Since we are interested in what happens locally around $b = 1$, $\varphi = 3\pi/2$, we need to know the bifurcation set in the adjoining region, where $\varphi \in [3\pi/2, 2\pi]$. This is just the known bifurcation set from Figure 1 rotated by 180° around $\varphi = 3\pi/2$, $\alpha = \pi/2$. Applying the transformation $(z, t) \mapsto (\bar{z}, -t)$ to the phase portraits in regions 1–15 of Figure 3 gives the respective phase portraits. Some of the phase portraits for $\varphi \in [3\pi/2, 2\pi]$ are topologically equivalent to phase portraits for $\varphi \in [\pi, 3\pi/2]$. Using a notation motivated by the above transformation we have: $9 = -\overline{4}$, $10 = -\overline{2}$, $14 = -\overline{12}$ and $13 = -\overline{15}$. (For example, applying $(z, t) \mapsto (\bar{z}, -t)$ to a phase portrait of type 4 gives a phase portrait of type 9.)

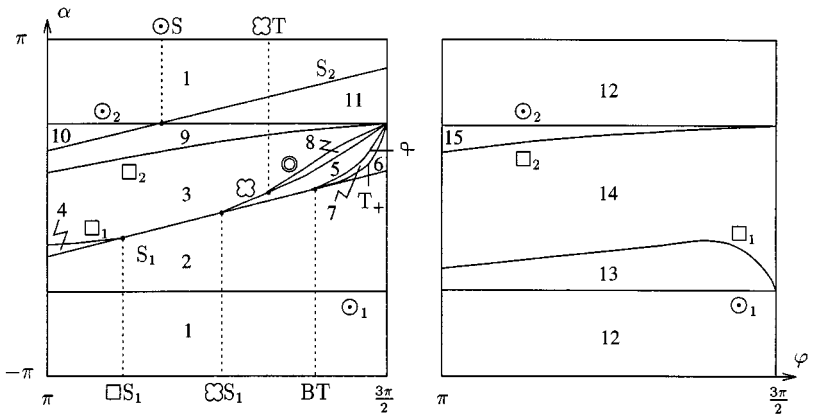

FIGURE 3. Sketches of two cross-sections of the bifurcation set with the symbols for the surfaces and curves and the numbering of the regions of phase portraits. Left: $b \approx 0.8$, right: $b > 1$; compare Figure 1 and see Table 1 for an explanation of the symbols.

3. *Characteristic neighborhoods*

Bifurcations at ∞ of (2) come into play for the following reason. The ultimate goal is to show that the principal part (1) contains all versal unfoldings. One needs to study unfoldings (for a fixed nonlinearity given by A and B) in a neighborhood of the origin in phase space for a small unfolding parameter ε. It is a general problem to define a suitable neighborhood of the origin, called the *characteristic neighborhood*, to which attention is restricted; compare [**DR93**, **DRSZ91**]. For example, equilibria or limit cycles can leave the characteristic neighborhood, which has to be regarded as a bifurcation.

In the present case the situation is as follows. We have scaled (1) to get (2), which in particular meant that we replaced a small ε by $e^{i\alpha}$ and consider α as a new parameter. The idea behind this is that an unfolding for small ε is determined by its bifurcation sequence when α is varied. In order to scale the modulus of ε to one, we first scale time by $1/|\varepsilon|$ and then the phase plane by $1/\sqrt{|\varepsilon|}$. Consequently, phenomena that occur in a neighborhood of the origin for small ε of the unscaled equation (1), can occur anywhere in the phase space $\mathbb{C}$ of the scaled equation (2). Alternatively, any point in the phase space $\mathbb{C}$ of the scaled equation (2) can be brought into an arbitrary neighborhood of the origin of the unscaled equation (1) by such a scaling. So, when replacing ε with $\varepsilon = e^{i\alpha}$ we can no longer restrict to a characteristic neighborhood, but have to consider the whole plane $\mathbb{C}$.

When certain boundary curves in the (b, φ)-plane are approached, equilibria or limit cycles escape off to infinity. This topological change of the phase portraits of (2) can be described by *bifurcations at* ∞, that is, by bifurcations on the boundary of the Poincaré disc. It is our aim to show that these bifurcations unfold versally in (2) and, consequently, do not give rise to yet unknown surfaces of codimension-one bifurcations in the bifurcation set. This constitutes a step towards proving that our model of the bifurcation set is complete, which, by the procedure of drilling, is evidence in support of Conjecture 1.

4. *The Hopf bifurcation revisited*

This section consists of a single example to illustrate our approach and the scalings involved. Consider the principal part (1) for $B = 0$ (when the purely $\mathbb{Z}_4$-symmetric part vanishes):

$$\dot{z} = \varepsilon z + Az|z|^2, \tag{4}$$

where $\varepsilon \in \mathbb{C}$ is an unfolding parameter and $A \in \mathbb{C}$ is a constant. This S^1-equivariant equation can be regarded as an unusual way of writing the Hopf bifurcation.

We treat (4) in complete analogy to the general case $B \neq 0$, that is, we are interested in all equivalence classes of unfoldings for small ε for generic A. Assuming $A \neq 0$, scaling phase space and time allows us to study

$$\dot{z} = e^{i\alpha} z + e^{i\varphi} z|z|^2, \tag{5}$$

where $\alpha \in (-\pi, \pi]$ and $\varphi \in (0, 2\pi]$. Due to the scaling the whole phase space $\mathbb{C}$ must be considered.

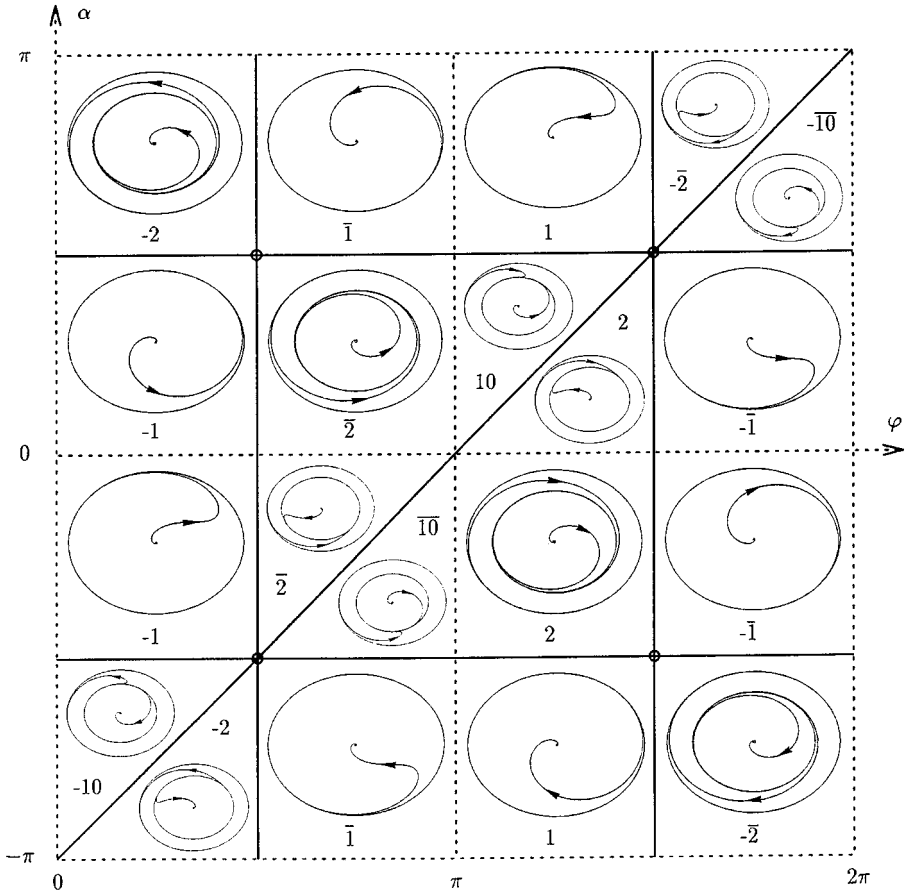

FIGURE 4. The Hopf bifurcation revisited. We call (φ, α)-space of (4) the 'magic torus'. Phase portraits are shown on the Poincaré disc, the outer circle representing ∞. They transform into each other by the symmetries $(z, t) \mapsto (\bar{z}, t)$ and $(z, t) \mapsto (\bar{z}, -t)$ as indicated by the labeling.

Consider the bifurcation set of (5) in the two-dimensional (φ, α)-space. Hopf bifurcations occur for $\alpha = \pm\pi/2$. For $\varphi = \alpha + \pi$ there is a circle of equilibria. The system is Hamiltonian for $\varphi = \pi/2$, $\alpha = \pm\pi/2$ and $\varphi = 3\pi/2$, $\alpha = \pm\pi/2$. This means that the genericity condition on the nonlinearity is $\varphi \neq \pm\pi/2$, which can be interpreted as follows. If φ passes through $\pi/2$ or $3\pi/2$ for $\alpha \neq \pm\pi/2$ a limit cycle disappears to infinity which clearly changes the topology of the phase portraits in $\mathbb{C}$.

We analyse this bifurcation by transforming ∞ of the phase plane into the origin by the change of coordinates $w = 1/z$ (where we take ∞ to be a point), which gives

$$\dot{w} = e^{i(\varphi+\pi)}w + e^{i(\alpha+\pi)}w|w|^2.$$

The roles of φ and α are exchanged which shows that for $\varphi = \pm\pi/2$ there are Hopf bifurcations at 0 in this new equation, the type of which depends on the choice of α. We call this bifurcation a Hopf bifurcation at ∞ of (5). In other words, for the original equation (4) the lines $\varphi = \pm\pi/2$, where the genericity condition is violated, are lines of Hopf bifurcations at ∞.

Figure 4 shows the bifurcation set of (5) in (φ, α)-space. Drilling in the direction of α for given φ gives the bifurcation sequence of (5) near the origin; drilling in the direction of φ for given α gives the bifurcation sequence near ∞. The solid horizontal lines correspond to Hopf bifurcations at the origin and the solid vertical lines to Hopf bifurcations at ∞. At the intersection points of these solid lines the system is Hamiltonian.

Typical phase portraits of (5) are shown on the Poincaré disc, where ∞ is not seen as a point, but is represented by the outer circle. They are transformed into each other by the symmetries $(z, t) \mapsto (\bar{z}, t)$ and $(z, t) \mapsto (\bar{z}, -t)$ as indicated, when the figure is rotated by 180° around $\varphi = \pi, \alpha = 0$ and $\varphi = 3\pi/2, \alpha = \pi/2$, respectively. Due to these symmetries we can restrict our attention to $\varphi \in [\pi, 3\pi/2]$. All this structure prompted us to call (φ, α)-space of (5) the *magic torus*.

Note that when studying the Hopf bifurcation one usually chooses $A = \pm 1$, which means that there is no rotation at ∞ since A is real. Furthermore, one is only interested in the behavior close to the bifurcation points where $\operatorname{Re}\varepsilon$ changes sign.

We remark that the bifurcation set of (2) for b close to zero can be seen as a singular perturbation of the magic torus. This point of view is under investigation and will be discussed elsewhere.

5. *The equations at ∞*

We return to the general context of studying the bifurcations at ∞ of (2). To this end we blow up ∞ as follows. Writing $z = re^{i\theta}$, we transform (2) to polar coordinates

$$\dot{r} = \cos\alpha\, r + (\cos\varphi + b\cos 4\theta)r^3, \quad \dot{\theta} = \sin\alpha + (\sin\varphi - b\sin 4\theta)r^2.$$

Substituting $\tilde{r} = 1/r$, dividing out the $\mathbb{Z}_4$-symmetry, multiplying by $\tilde{r}^2$ and dropping the tilde gives

$$\dot{r} = -\cos\alpha\, r^3 - (\cos\varphi + b\cos\theta)r, \quad \dot{\theta} = 4(\sin\alpha\, r^2 + (\sin\varphi - b\sin\theta)).$$

Since we are interested in the case $(b, \varphi) = (1, 3\pi/2)$ we shift $\tilde{\theta} = \theta + \pi/2$ to get $(r, \tilde{\theta}) = (0, 0)$ as the central singularity. Again, dropping the tilde gives

$$\dot{r} = -(\cos\varphi + b\sin\theta)r - \cos\alpha\, r^3, \quad \dot{\theta} = 4(\sin\varphi + b\cos\theta) + 4\sin\alpha\, r^2,$$

which is (3). The planar vector field (3) has the reflectional symmetry $r \mapsto -r$ and the translational symmetry $\theta \mapsto \theta + 2\pi$. By dividing out these symmetries we get a vector field on the half-cylinder $\mathbb{R}^+ \times \mathbb{R}/2\pi\mathbb{Z}$. Since we are interested in the singularity at $(r, \theta) = (0, 0)$ it is convenient to choose θ from $(-\pi, \pi]$. Alternatively, (3) can be regarded as a vector field on the covering space $\mathbb{R}^2$.

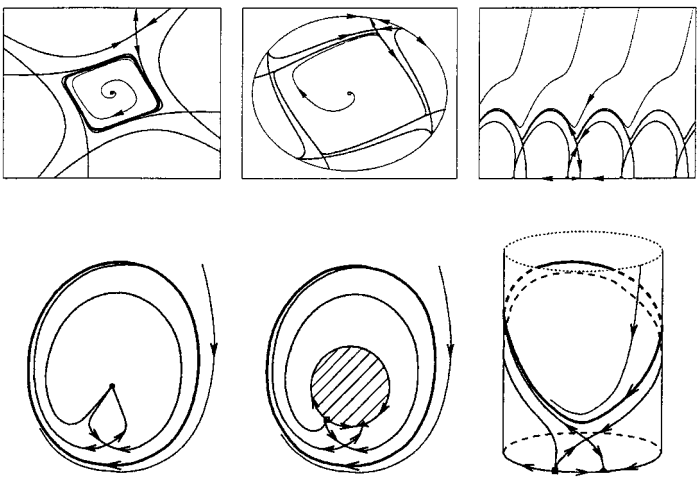

FIGURE 5. The blow-up of ∞ interpreted in two ways. (The example is 13 from Figure 3.) Top row: phase portraits generated with DsTool and containing the $\mathbb{Z}_4$-symmetry; left: on $\mathbb{C}$; middle: on the Poincaré disc; right: the Poincaré disc written in polar coordinates gives (3). Bottom row: sketches with the symmetry divided out; left: ∞ brought to the origin; middle: the blow-up of the origin; right: the blow-up (3) on the half-cylinder $\mathbb{R}^+ \times (-\pi, \pi]$. The top right panel is the four-fold cover of the half-cylinder.

We have divided out the original $\mathbb{Z}_4$-symmetry for convenience in the calculations. However, one gets another interpretation of the blow-up we performed by considering (3) on the four-fold cover $\mathbb{R}^+ \times \mathbb{R}/8\pi\mathbb{Z}$, thereby restoring the $\mathbb{Z}_4$-symmetry. The vector field on the four-fold cover can be seen as the original vector field (2) on the Poincaré disc, written in polar coordinates. The different viewpoints are illustrated in Figure 5.

Note that $\{r = 0\}$ is an invariant circle of (3), or an invariant line if we think of the cover, representing ∞ in (2). (For the vector field on the Poincaré disc, $\{r = 1\}$ is the invariant circle representing ∞.) We call a bifurcation at $\{r = 0\}$ of (3) a *bifurcation at* ∞ of (2). From now on, when we talk about the codimension of a singularity or bifurcation we mean the codimension in the class of reflectionally symmetric planar vector fields, where the symmetry group is $\mathbb{Z}_2$, generated by $(r, \theta) \mapsto (-r, \theta)$.

6. *Codimension-one bifurcations*

As mentioned earlier we investigate (3) in (b, φ, α)-space, where $\varphi \in [\pi, 2\pi]$. For the codimension-one bifurcations we have the following.

THEOREM 3. *There are the following surfaces of codimension-one bifurcations of (3) on the invariant circle $\{r = 0\}$. (For the notation see Table 1.)*

(a) *A surface S^∞ of saddle-node bifurcations, given by $b = |\sin\varphi|$. The equilibria at $\{r = 0\}$ occur for $b > |\sin\varphi|$.*

(b) *A surface $\pitchfork^\infty$ of pitchfork bifurcations, given by $b = 1$. This surface is divided into two parts by the lines $\alpha = \varphi - \pi \pm \pi/2$, where $\pitchfork^\infty$ intersects the surfaces S_1 and S_2. A pitchfork bifurcation for the part where $\alpha \in (\varphi - \pi - \pi/2, \varphi - \pi + \pi/2)$ yields equilibria outside the invariant circle for $b < 0$, for the other part it yields equilibria outside the invariant circle for $b > 0$. For $\varphi = 3\pi/2$ the pitchfork bifurcation is transcritical.*

(c) *A surface $\odot^\infty$ of Hopf bifurcations, that is, of limit cycle bifurcations at $\{r = 0\}$, given by $\varphi = 3\pi/2$, $b \in (0, 1)$. This surface is divided into two parts by the lines $\alpha = \pm\pi/2$, where the system has infinitely many closed orbits. For $\alpha \in (-\pi/2, \pi/2)$ the Hopf bifurcation is supercritical and for $\alpha \in (-\pi, -\pi/2) \cup (\pi/2, \pi)$ it is subcritical.*

Proof. (a) For $\{r = 0\}$ there are equilibria if $|\sin\varphi/b| \leq 1$. Consequently, saddle-node bifurcations occur for $b = |\sin\varphi|$.

(b) There is a pitchfork bifurcation at $\{r = 0\}$ if there is an equilibrium with a neutral direction. This is the case if we have for some θ that

$$\cos\theta = \frac{-\sin\varphi}{b} \quad \text{and} \quad \sin\theta = \frac{-\cos\varphi}{b}.$$

Taking the sum of the squares of the above equation gives

$$b^2 = \sin^2\varphi + \cos^2\varphi = 1$$

and we conclude that $b = 1$ since $b \in \mathbb{R}^+$.

The intersection with the surfaces S_1 and S_2 is immediate. This gives the partition of $\pitchfork^\infty$ into the two parts as stated; compare the circle construction in [**Kra94b**].

Suppose that $\varphi \in [\pi, 3\pi/2)$ and $b < 1$. Keeping in mind that $\cos\varphi < 0$, this gives for the bifurcating equilibrium θ_0 on the invariant circle $\{r = 0\}$,

$$\cos\varphi + b\sin\theta_0 = \cos\varphi + b\sqrt{1 - \cos^2\theta_0} = \cos\varphi + \sqrt{b^2 - \sin^2\varphi} < 0.$$

This shows that θ_0 is repelling for $b < 1$ and $\varphi \in [\pi, 3\pi/2)$, and analogously one shows that θ_0 is attracting for $b > 1$ and $\varphi \in [3\pi/2, 2\pi)$. We conclude that along the line $\varphi = 3\pi/2$ the pitchfork bifurcation is transcritical.

(c) For $\varphi = 3\pi/2$ we have

$$\dot r = -b\sin\theta\, r - \cos\alpha\, r^3, \quad \dot\theta = 4(b\cos\theta - 1) + 4\sin\alpha\, r^2. \tag{6}$$

Provided $b < 1$ there are no equilibria on the invariant circle. The difficulty is that $\dot\theta$ depends on θ. This is different from the trivial example in §4, where the Hopf bifurcation at ∞ could be completely analysed by bringing ∞ to the origin. In the present situation one needs to calculate the coefficients of the Poincaré map on a section perpendicular to the invariant circle. We use the results in [**BR93**], where a criterion is given for a

generic bifurcation of a limit cycle in a system like (6). Using the notation from [**BR93**] we write $dr/d\theta = \alpha_1 r + \alpha_2 r^2 + \alpha_3 r^3 + \cdots$ and conclude from (6) that

$$\alpha_1 = \frac{-b\sin\theta}{4(b\cos\theta - 1)}, \quad \alpha_2 = 0, \quad \alpha_3 = \frac{-\cos\alpha}{4(b\cos\theta - 1)} + \frac{b\sin\alpha\sin\theta}{4(b\cos\theta - 1)^2}.$$

We need to calculate the functions

$$\begin{aligned} u_1(\theta) &= \exp\left(\int_0^\theta \alpha_1(\tau)\,d\tau\right) = \left(\frac{1 - b\cos\theta}{1 - b}\right)^{1/4}, \\ u_2(\theta) &= u_1(\theta)\int_0^\theta \alpha_2(\tau)u_1(\tau)\,d\tau \equiv 0, \end{aligned}$$

and

$$u_3(\theta) = u_1(\theta)\int_0^\theta (2\alpha_2(\tau)u_2(\tau) + \alpha_3(\tau)u_1^2(\tau))\,d\tau.$$

This gives

$$u_1(2\pi) = 1, \quad u_2(2\pi) = 0$$

and

$$u_3(2\pi) = \frac{\cos\alpha}{4\sqrt{1-b}}\int_0^{2\pi} \frac{d\tau}{(1 - b\cos\tau)^{1/2}}.$$

The sign of $u_3(2\pi)$ is determined by the sign of $\cos\alpha$ and the result follows from Theorem 2.1 of [**BR93**], the criterion for the generic limit cycle bifurcation. There are infinitely many closed orbits for $\alpha = \pm\pi/2$, since this is the Hamiltonian case of (2). We remark that in this case we have $\dot\theta = 4((b\cos\theta - 1) \pm r^2)$, which allows us to check if the closed orbits occur near the invariant circle $\{r = 0\}$ or not by considering the zeros for small r. For $b < 1$ there are infinitely many closed orbits near $\{r = 0\}$ and for $b > 1$ there are none near $\{r = 0\}$. □

Remark 4. We denote the surfaces in Theorem 3 by S^∞, $\curlywedge^\infty$ and $\odot^\infty$ to indicate that we think of them as bifurcations at ∞ of (2). We call the limit cycle bifurcation along $\odot^\infty$ a Hopf bifurcation at ∞, because we think of ∞ as a point in terms of the original problem.

Remark 5. The surfaces $\curlywedge^\infty$ and $\odot^\infty$ are part of the bifurcation set and lead to boundary curves in the (b, φ)-plane of (2); compare Figure 2. Note that the surface $\odot^\infty$ is nonlocal (in the sense that it is not given by conditions on equilibria), but that it has an analytic expression.

The surface S^∞ is *not* part of the bifurcation set and does not lead to a boundary curve in the (b, φ)-plane of (2). This is so because a saddle-node bifurcation at ∞ does not change the equivalence type of a phase portrait in the phase space $\mathbb{C}$ of (2).

7. *The singularities for $b = 1, \varphi = 3\pi/2$*

Already from Theorem 3 it is clear that the line $b = 1$, $\varphi = 3\pi/2$, $\alpha \in (-\pi, \pi]$ is interesting since it is the intersection of the surfaces S^∞, $\curlywedge^\infty$ and $\odot^\infty$. Furthermore, several surfaces of the bifurcation set accumulate on it; see Figure 1. From theoretical and numerical results we get the following.

OBSERVATION 6. *For $b = 1$, $\varphi = 3\pi/2$ and any α the point $(r, \theta) = (0, 0)$ is an equilibrium of system (3) with zero Jacobian, that is*

$$D_{1,3\pi/2,\alpha}(0,0) = \begin{pmatrix} 0 & 0 \\ 0 & 0 \end{pmatrix}.$$

Furthermore, we have the following:

(a) *for $\alpha \notin \{0, \pm\pi/2, \pi\}$ the singularity is of at least codimension two;*

(b) *for $\alpha \in \{0, \pi\}$ the singularity is of at least codimension three;*

(c) *for $\alpha = \pm\pi/2$ the system has infinitely many closed orbits.*

Remark 7. The sign of $\cos\alpha$ in (3) can be reversed by the coordinate change $(r, \tilde{\theta}, b, \tilde{\varphi}, \tau) = (r, -\theta, b, 3\pi/2 - \varphi, -t)$. As a consequence we can restrict our attention to the case $\cos\alpha \geq 0$, that is, to $\alpha \in [-\pi/2, \pi/2]$.

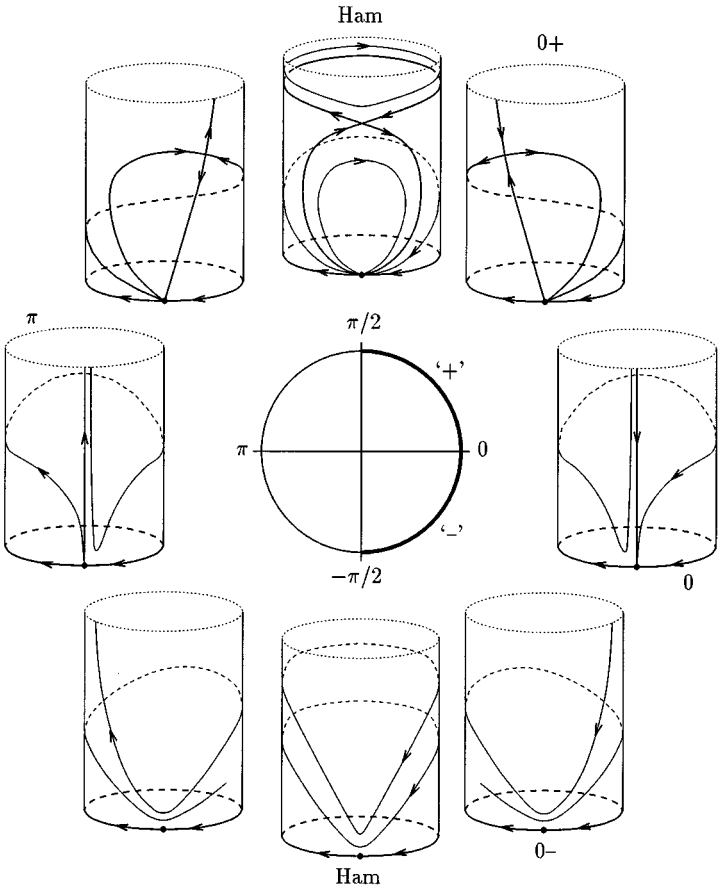

FIGURE 6. The degenerate phase portraits of the vector field (3) on the cylinder for $b = 1$ and $\varphi = 3\pi/2$.

The idea in the remainder of this section is to show that the singularities of Observation 6 unfold versally in (3). To give an idea of these singularities Figure 6 shows phase portraits of (3) for $b = 1$, $\varphi = 3\pi/2$ and varying α grouped around the circle $e^{i\alpha}$.

First we unfold the singularities of Observation 6(a). We regard α as a constant and (b, φ) as the unfolding parameters. (This exchange in the roles between α and (b, φ) constitutes another justification to give up the original distinction between parameters and constants.) It turns out that unfoldings for two different values of α from one of the intervals $(-\pi/2, 0)$ and $(0, \pi/2)$ are equivalent. Hence, there are exactly two different cases, which we denote case '$-$' and case '$+$', respectively, depending on the sign of $\sin\alpha$. We show that these singularities unfold versally in the parameters b and φ, when one restricts to phenomena that occur in a neighborhood of the singularity $(r, \theta) = (0, 0)$. In particular, the singularities are indeed of codimension two. Furthermore, we discuss how global phenomena, such as limit cycles and heteroclinic connections, tend to a limit as (b, φ) tends to $(1, 3\pi/2)$.

The next question we tackle is the unfolding of the singularity for $\alpha = 0$, which gives the connection between case '$-$' and case '$+$'. The point $b = 1$, $\varphi = 3\pi/2$, $\alpha = 0$ is an organizing center: arbitrarily close to it one finds all regions of phase portraits (where the transformation $(z, t) \mapsto (\bar{z}, -t)$ is taken into account). We give an unfolding of this singularity in the parameters (b, φ, α), where we again restrict to phenomena that occur in a neighborhood of $(r, \theta) = (0, 0)$. Together with numerical data on global phenomena this gives a complete picture of the organizing center.

Note that the Hamiltonian lines $\varphi = 3\pi/2$ and $\alpha = \pm\pi/2$ are fixed under the symmetry $(z, t) \mapsto (\bar{z}, -t)$. This is why the structure of the bifurcation set around the points $b = 1$, $\varphi = 3\pi/2$, $\alpha = \mp\pi/2$ is immediate from this symmetry and the knowledge of case '$-$' and case '$+$', respectively. The Hamiltonian cases along these lines have been studied in [**Nei78**].

8. *Case '$-$' and case '$+$'*

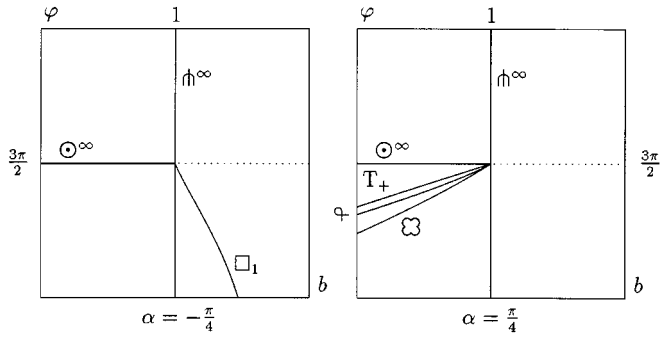

FIGURE 7. Cross-sections of the bifurcation set computed by continuation with AUTO. Left: the case '$-$' ($\alpha = -\pi/4$ in the computations). Right: the case '$+$' ($\alpha = \pi/4$ in the computations). The curve ◎ is not included since it is extremely close to ♡. It is, however, present in the sketches of Figures 10 and 11. For the notation see Table 1.

In this section α is fixed and b and φ are unfolding parameters. An unfolding for a given α can be obtained from the bifurcation set of (2) by considering a cross-section for this value of α locally around $b = 1$, $\varphi = 3\pi/2$. Figure 7 shows cross-sections of the bifurcation set for the two cases computed by continuing the respective codimension-one

bifurcations with the continuation package AUTO; see [**Doe86**]. In the calculations we used $\alpha = -\pi/4$ for case '$-$', and $\alpha = \pi/4$ for case '$+$'. Figure 7 illustrates how the curves $\square_1$, T_+, φ and $\boxtimes$ tend to the point $b = 1,\ \varphi = 3\pi/2$. Note that the curve $\circledcirc$ is very close to $\boxtimes$ and is not shown in the figure. The curve S^∞ is not present since it is not part of the bifurcation set.

Figures 8–11 show the bifurcation diagrams for case '$-$' and case '$+$'. Typical phase portraits, calculated with DsTool (see [**BGMWW92**]), are grouped around a sketch of the bifurcation set (which now contains the curve S^∞). This is done in two different ways: by showing (2) on the Poincaré disc, and by showing (3) on the four-fold cover of the half-cylinder; compare Figure 5. The phase portraits on the Poincaré disc (the outer circle represents ∞) give the connection with the generic phase portraits of (2) on $\mathbb{C}$. For the four-fold cover the angle θ is the horizontal direction and the radial component r is the vertical direction. The invariant circle $\{r = 0\}$, corresponding to infinity and the boundary of the Poincaré disc, is at the bottom of the pictures. The advantage of showing (3) on the cover is that global phenomena, such as limit cycles and heteroclinic connections, are easier to see. Furthermore, it emphasizes the original $\mathbb{Z}_4$-equivariance.

It is in the logic of bifurcation theory to distinguish *local features*, which occur in a small neighborhood of $(r, \theta) = (0, 0)$ for the parameters near $b = 1,\ \varphi = 3\pi/2$, and *global features*, which do not. We first discuss the singularities for case '$-$' and case '$+$' from the local point of view. In this analysis it is not important that (3) is defined on a half-cylinder.

THEOREM 8. *For any given $\alpha \notin \{0, \pm\pi/2, \pi\}$ equation (3) is a versal unfolding in a neighborhood of the singularity $(r, \theta, b, \varphi) = (0, 0, 1, 3\pi/2)$.*

Proof. According to Remark 7 we can restrict the study to case '$-$', where $\alpha \in (-\pi/2, 0)$, and case '$+$', where $\alpha \in (0, \pi/2)$. The idea of the proof is to show that (3) is a perturbation of a versal unfolding of a reflectionally equivariant planar vector field with Jacobian equal to zero. These unfoldings can be found, for example, in [**AAIS86**, **CLW94**, **GH86**].

In a small neighborhood of the singularity we may use the Taylor series expansions for $\cos\theta$ and $\sin\theta$ in (3). Ordering in powers of r and θ yields

$$\dot r = -\cos\varphi\, r - br\theta - \cos\alpha\, r^3 + O(|r,\theta|^4), \quad \dot\theta = 4(\sin\varphi + b) + 4\sin\alpha\, r^2 - 2b\theta^2 + O(\theta^4), \tag{7}$$

giving the singularity

$$\dot r = -br\theta - \cos\alpha\, r^3 + O(|r,\theta|^4), \quad \dot\theta = 4\sin\alpha\, r^2 - 2b\theta^2 + O(\theta^4).$$

The last equation is a special case of Equation (7.4.2) in [**GH86**, p. 377] with $a_1 = -b,\ a_2 = -\cos\alpha,\ a_3 = 0,\ b_1 = 4\sin\alpha,\ b_2 = -2b,\ b_3 = b_4 = 0$. This system is two-determined since $a_1, b_1, b_2 \neq 0$ and $b_2 - a_1 = -b \neq 0$ (compare [**Ta74a**]) and is equivalent to the normal form

$$\dot r = -\tfrac{1}{2} r\theta, \quad \dot\theta = \pm r^2 - \theta^2. \tag{8}$$

In the following lines we check that (7) is a versal unfolding by calculating the unfolding parameters. Rescaling time $\tau = 2t$ and plugging in the Taylor series expansions of $\sin\varphi$

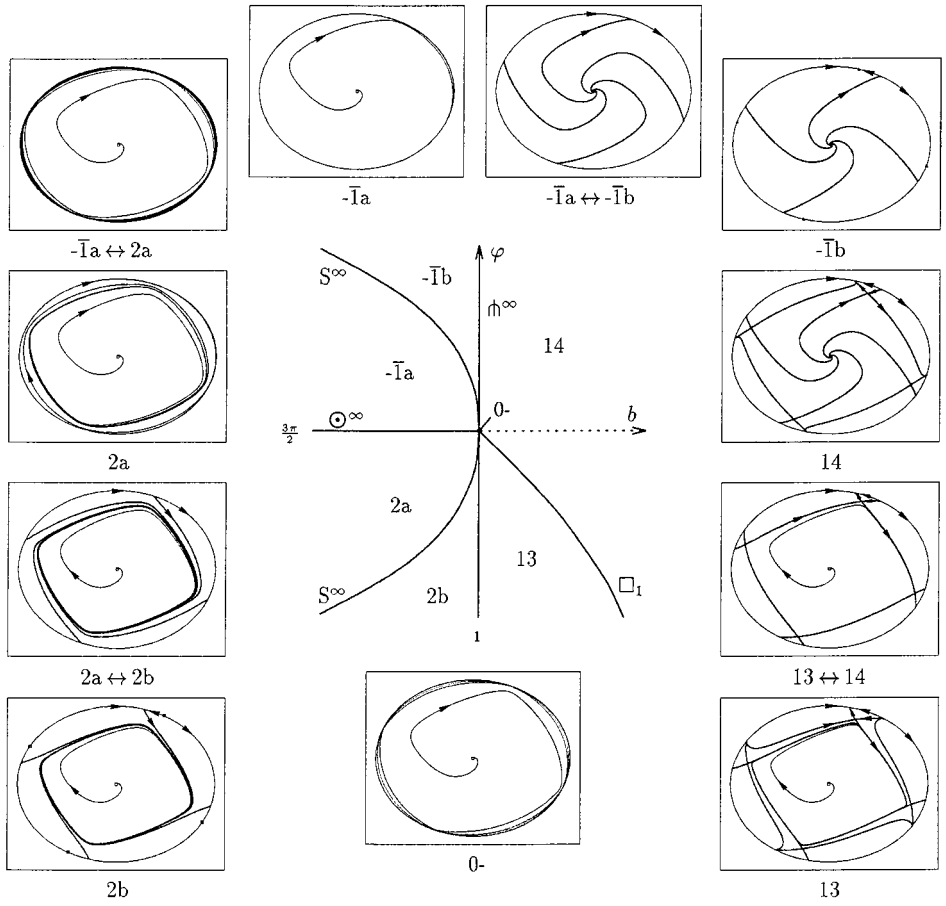

FIGURE 8. The bifurcation diagram of (2) for the case '−' ($\alpha = -\pi/4$ in the computations). The phase portraits are shown on the Poincaré disc to illustrate the bifurcations at ∞, represented by the outer circle.

and $\cos\varphi$ around $\varphi = 3\pi/2$ gives

$$\begin{aligned}\dot{r} &= \frac{1}{2}\left(\left(\varphi - \frac{3\pi}{2}\right) - \left(\varphi - \frac{3\pi}{2}\right)^3/6 + \cdots\right) r - \frac{1}{2} b r\theta - \frac{1}{2}\cos\alpha\, r^3 + O(|r,\theta|^4)\\ \dot{\theta} &= 2\left((b-1) + \left(\varphi - \frac{3\pi}{2}\right)^2/2 - \cdots\right) + 2\sin\alpha\, r^2 - b\theta^2 + O(\theta^4).\end{aligned}$$

Setting $\mu_1 = (\varphi - 3\pi/2)/2$ and $\mu_2 = 2(b-1) + 4\mu_1^2$ gives

$$\begin{aligned}\dot{r} &= \mu_1 r - \tfrac{1}{2} r\theta - \tfrac{1}{2}\cos\alpha\, r^3 + O(\mu_1^3 r, \mu_2 r\theta, \mu_1^2 r\theta, |r,\theta|^4)\\ \dot{\theta} &= \mu_2 + 2\sin\alpha\, r^2 - \theta^2 + O(\mu_1^4, \mu_2\theta^2, \mu_1^2\theta^2, \theta^4).\end{aligned} \tag{9}$$

Rescaling $\tilde{r} = \sqrt{|2\sin\alpha|}\, r$ for given $\alpha \neq 0$ yields, after dropping the tilde,

$$\begin{aligned}\dot{r} &= \mu_1 r - \tfrac{1}{2} r\theta - \tfrac{1}{4}|\cot\alpha| r^3 + O(\mu_1^3 r, \mu_2 r\theta, \mu_1^2 r\theta, |r,\theta|^4)\\ \dot{\theta} &= \mu_2 \pm r^2 - \theta^2 + O(\mu_1^4, \mu_2\theta^2, \mu_1^2\theta^2, \theta^4),\end{aligned}$$

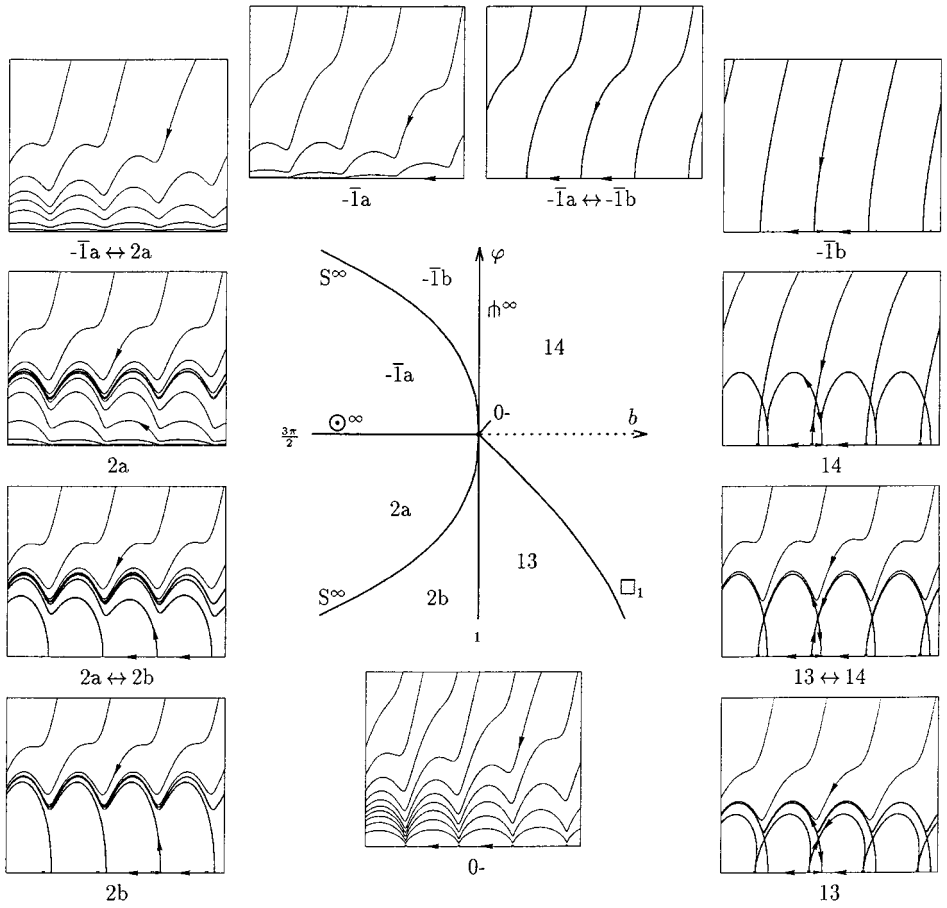

FIGURE 9. The bifurcation diagram of (3) for the case '$-$', ($\alpha = -\pi/4$ in the computations). In the panels of the phase portraits, θ is the horizontal and r the vertical direction. The lower boundary of the pictures is the invariant line $\{r = 0\}$ representing ∞.

where $\pm$ is the sign of α. This shows that (3) is a small perturbation of the versal unfolding of (8) in a neighborhood of $(r, \theta, b, \varphi) = (0, 0, 1, 3\pi/2)$. Since the coefficient of $r\theta$ is $-\frac{1}{2}$, only the cases IIa and IVa in Figure 7.4.1 of [**GH86**, p. 379] can occur, depending on the sign of $b_1 = 4\sin\alpha$. In particular, all unfoldings for α from $(-\pi/2, 0)$, and all unfoldings for α from $(0, \pi/2)$ are indeed topologically equivalent, justifying that we speak of case '$-$' and case '$+$'.

The versal unfoldings are shown in Figure 12 for case '$-$' and case '$+$'; compare the figures in [**AAIS86**, p. 26] and Figures 7.4.4. and 7.4.6. in [**GH86**, p. 384]. From a result of Żołądek one can conclude the following (see [**AAIS86**]). For case '$-$' there is no limit cycle, for case '$+$' there is exactly one limit cycle. (Note that we have $|\cot\alpha| \neq 0$.) This limit cycle is born in a Hopf bifurcation inside any characteristic neighborhood, but intersects its boundary as it grows. This must be considered a bifurcation: the vanishing of a limit cycle; see Figure 13. This bifurcation is of a local nature, globally

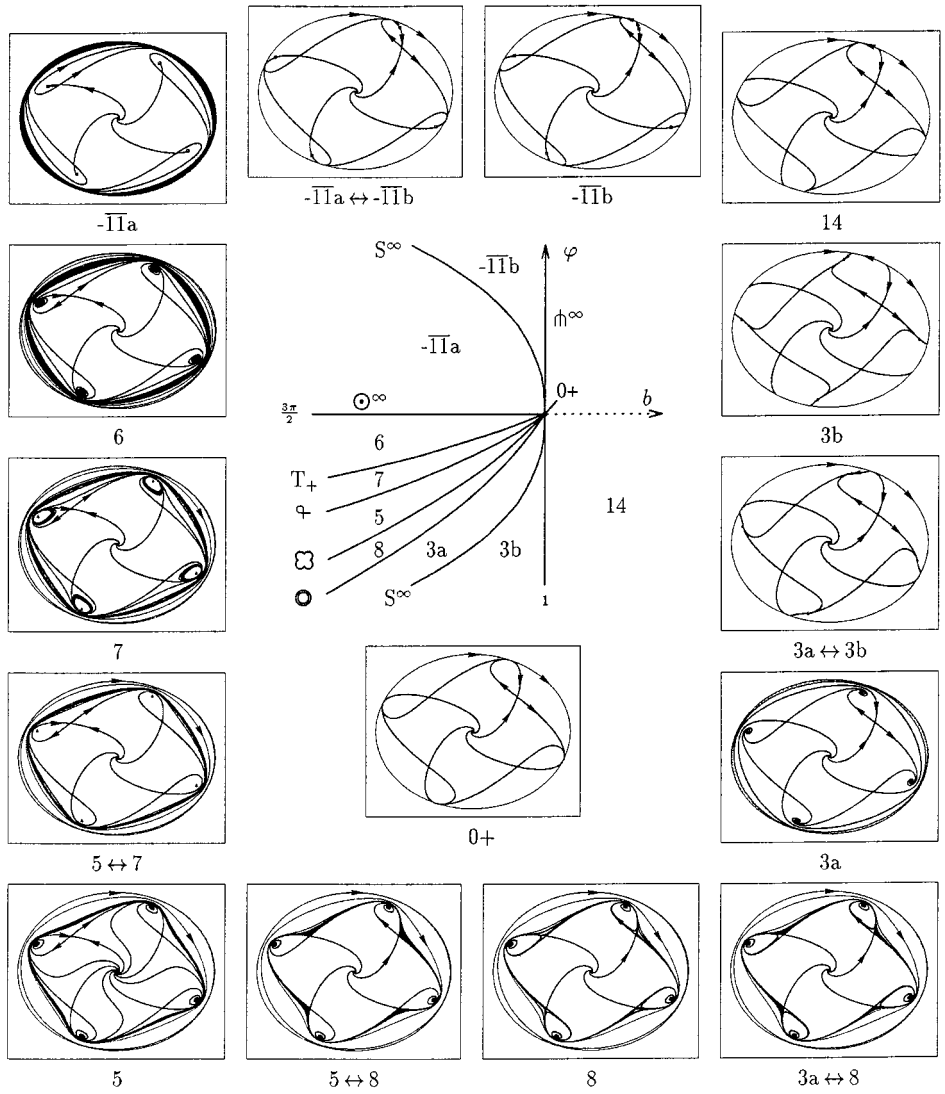

FIGURE 10. The bifurcation diagram of (2) for the case '+' ($\alpha = \pi/4$ in the computations). The phase portraits are shown on the Poincaré disc to illustrate the bifurcations at ∞, represented by the outer circle.

it is not a bifurcation. This is a well-known kind of problem in bifurcation theory; see [**DR93**, **DRSZ91**]. There is a curve N of points in parameter space for which the circle leaves the characteristic neighborhood, provided this neighborhood has a suitable shape. In the present case a certain disc would do. In general, it is a major problem that the shape of the characteristic neighborhood can be of importance. □

Theorem 8 has a drawback. Looking at Figures 8–11 makes it clear that most features of the phase portraits are global. For case '$-$' the saddle-node bifurcations S^∞ and the pitchfork bifurcations $\pitchfork^\infty$ can be found near $(r, \theta) = (0, 0)$. For case '$+$' one also

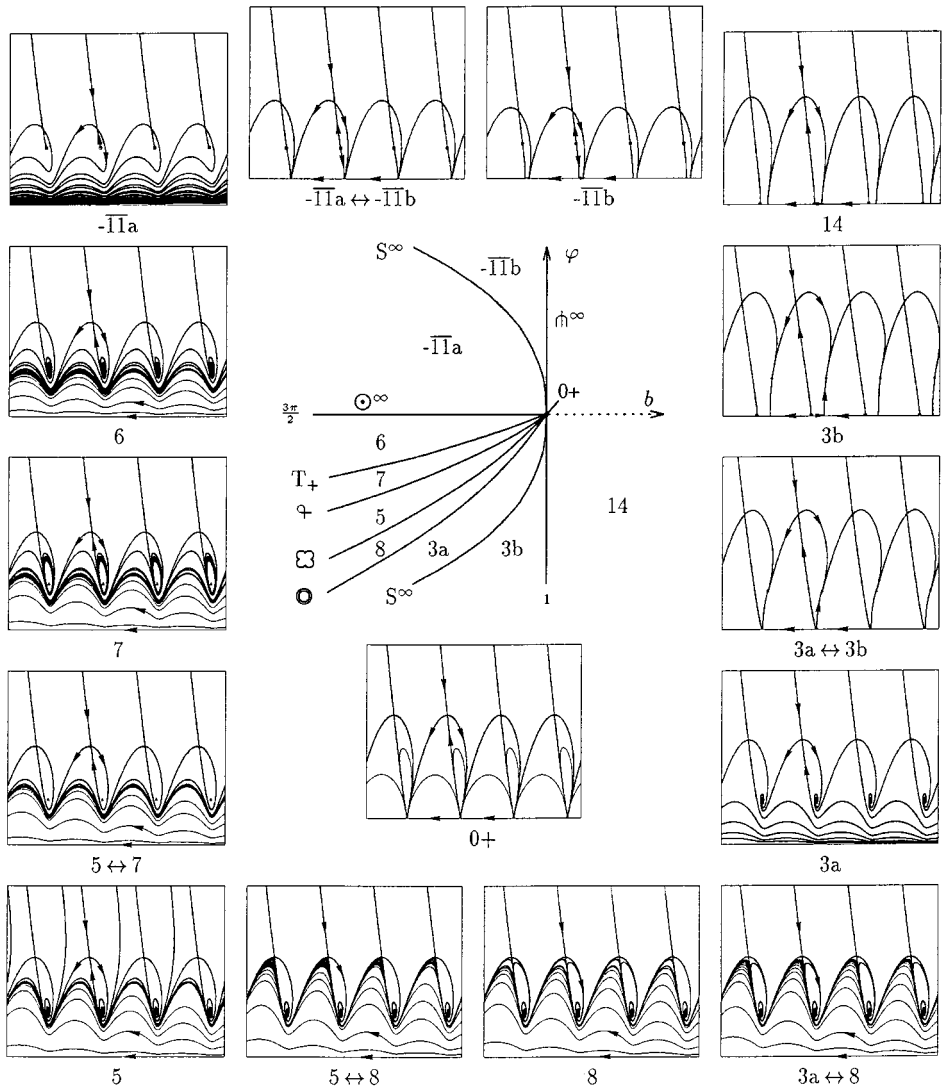

FIGURE 11. The bifurcation diagram of (3) for the case '+' ($\alpha = \pi/4$ in the computations). In the panels of the phase portraits, θ is the horizontal and r the vertical direction. The lower boundary of the pictures is the invariant line $\{r = 0\}$ representing ∞.

finds the curve ⊙ where the secondary equilibrium undergoes a Hopf bifurcation. The problem is that in this case there is a minimum distance (depending on α) between the invariant circle and the equilibrium furthest from the invariant circle. This means that the homoclinic connection ⍜ is not visible in a small neighborhood around $(r, \theta) = (0, 0)$. The same holds for a limit cycle around the secondary equilibrium if it is big, that is, if it passes sufficiently close to the saddle point. However, such a limit cycle can also be small since it is born in a Hopf bifurcation of the node, which can be found arbitrarily

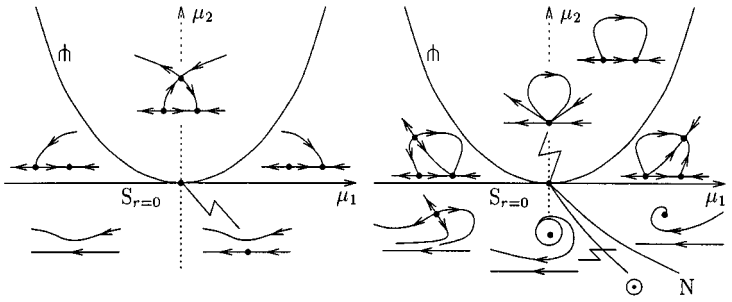

FIGURE 12. The versal unfoldings near $(r, \theta) = (0, 0)$ as given by (10). Left: the case '$-$'; right: the case '$+$'. Note that the limit cycle intersects the boundary of the characteristic neighborhood as the curve N is crossed; compare the figures in [AAIS94, pp. 26 and GH86, pp. 384].

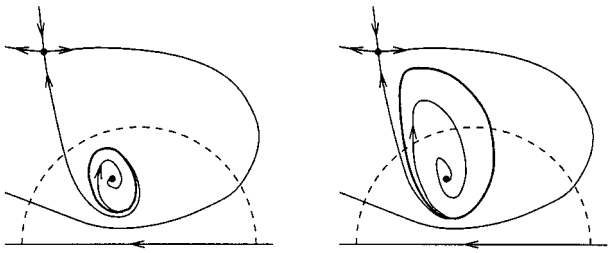

FIGURE 13. Left: a limit cycle is born in a Hopf bifurcation of secondary equilibria inside the characteristic neighborhood. Right: as the limit cycle grows it intersects the boundary, so that it is not detectable in the characteristic neighborhood.

close to $(r, \theta) = (0, 0)$. In short, some limit cycles are global and some are local, depending on the size and shape of the characteristic neighborhood under consideration; compare Figure 13.

The limit cycle bifurcating along $\odot^\infty$ cannot be detected near the singularity $(r, \theta) = (0, 0)$. This is not surprising since it goes once around the half-cylinder. The same holds for the heteroclinic connections $\square_1$ and $\boxtimes$ and the second limit cycle bifurcating from it. We call such phenomena, which are induced by the topology of the half-cylinder, *topologically global*. They need to be studied in a neighborhood of the entire invariant circle $\{r = 0\}$; see §10.

We conclude this section by studying what happens to topologically global phenomena as the point $b = 1,\ \varphi = 3\pi/2$ is approached for a given α. We want to see if one can find a characteristic neighborhood of the invariant circle, in which all topologically global phenomena remain, for (b, φ) sufficiently close to $(1, 3\pi/2)$. For case '$-$' there is exactly one limit cycle, namely the topologically global one bifurcating from the invariant circle along $\odot^\infty$. This limit cycle and the heteroclinic connection $\square_1$, in which it disappears, converge to the invariant circle as $b = 1,\ \varphi = 3\pi/2$ is approached. Hence, it is no problem to define a characteristic neighborhood of the invariant circle in this case.

The situation is entirely different for case '$+$'. Consider the topologically global limit

cycle bifurcating from the invariant circle along $\odot^{\infty}$, which vanishes in the saddle-node of limit cycle bifurcation ◎. The second topologically global limit cycle, with which it bifurcates, is born in the clover connection ⁂, that is, it lives close to the saddle point. Consequently, this one-parameter family of limit cycles converges to a one-parameter family of homoclinic connections of the degenerate point $(r, \theta) = (0, 0)$. (Any trajectory from the singularity $(r, \theta) = (0, 0)$ to itself around the cylinder can be the limit of a topologically global limit cycle, provided the point $b = 1,\ \varphi = 3\pi/2$ is approached along a suitable curve. Such a curve can be thought of as parameter values for which the limit cycle is a given distance away from the saddle.) In particular, the limit may be far from the invariant circle, so that it is impossible to find a characteristic neighborhood of $\{r = 0\}$.

The reason for the difficulty of defining suitable characteristic neighborhoods, both locally around $(r, \theta) = (0, 0)$ and around the invariant circle $\{r = 0\}$, comes from the fact that the saddle maintains a minimum distance from the invariant circle. This problem is overcome in the next section by studying the unfolding of the point $b = 1,\ \varphi = 3\pi/2,\ \alpha = 0$ in parameter space.

9. *An organizing center*

In this section $b,\ \varphi$ and α are parameters unfolding the singularity $(r, \theta) = (0, 0)$ for $b = 1,\ \varphi = 3\pi/2,\ \alpha = 0$, which gives a connection between case '$-$' and case '$+$'. The bifurcation diagram near this singularity in system (3) can be obtained from the bifurcation set by considering its structure near the point $b = 1,\ \varphi = 3\pi/2,\ \alpha = 0$, which can be studied by intersecting it with a small sphere around this point. Surfaces intersect the sphere in curves, which meet in points corresponding to curves of codimension-two bifurcations in the bifurcation set. Open regions on the sphere correspond to generic phase portraits.

We give a complete description of the bifurcation diagram on this sphere based on our knowledge of the bifurcation set and numerical investigations. Since we are interested in the bifurcations close to $(r, \theta) = (0, 0)$ we need to take the surface S^{∞} into account, which is not part of the bifurcation set of (2). Figure 14 shows the half of the sphere that intersects the region where $\varphi \in [\pi, 3\pi/2]$, which we call the *cube of interest*. The dashed curves indicate where the surface S^{∞} would intersect the bifurcation set. Figure 15 consists of three views of the sphere, where only the surfaces are drawn that are actually intersected. The sphere is shown from the exact same viewpoints in Figure 16 to give a good view of the boundary curves between the different regions of generic phase portraits.

In the last step we project the sphere stereographically onto the plane in the direction of φ. The half of the sphere in the cube of interest, see Figures 14 and 16 (right), is projected inside a circle, and the other half in the adjoining cube is projected outside this circle. Labeling the regions of generic phase portraits gives the bifurcation diagram depicted in Figures 17. The phase portraits of (3) are shown on the four-fold cover.

Figure 18 shows the bifurcation diagram of the original equation (2) on the projected sphere (the curve S^{∞} is not present any more) with the generic phase portraits in the phase space $\mathbb{C}$. All generic phase portraits occur, up to the transformation $(z, t) \mapsto (\bar{z}, -t)$.

(Recall that $9 = -\overline{4}$, $10 = -\overline{2}$, $14 = -\overline{12}$ and $13 = -\overline{15}$.) Figure 18 contains all essential information about (2) in an extremely condensed form. This is why we call the point $b = 1,\ \varphi = 3\pi/2,\ \alpha = 0$, the *organizing center* of (2). We believe that understanding the organizing center constitutes a major step towards proving Conjecture 1.

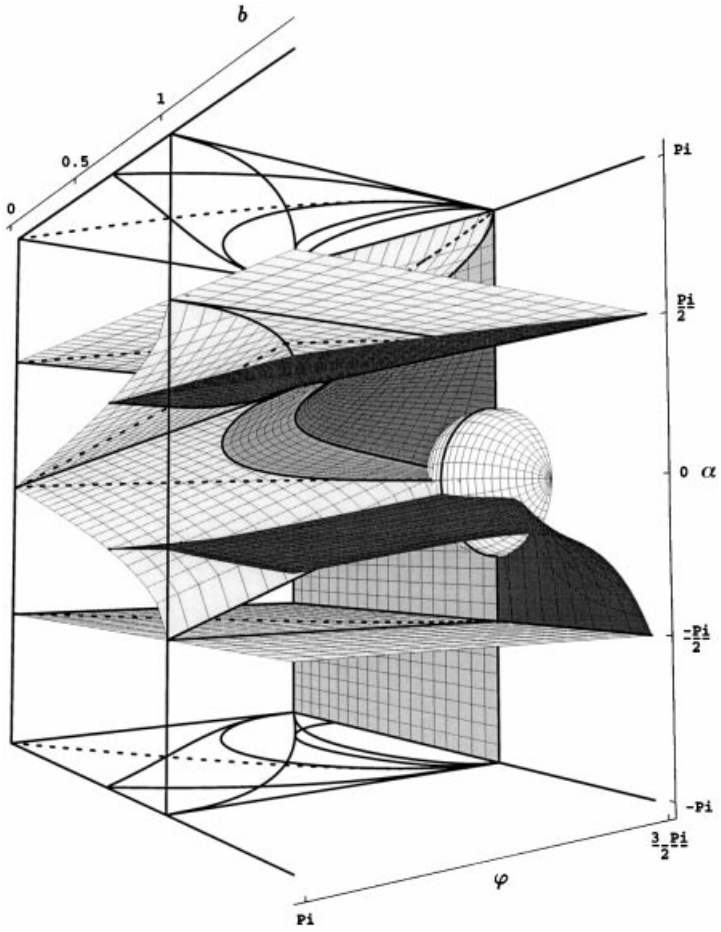

FIGURE 14. The bifurcation set intersected with a sphere around the organizing center $b = 1, \varphi = 3\pi/2$, $\alpha = 0$. Note that the surface $\pitchfork^{\infty}$, given by $b = 1$, is not shown and that some surfaces are hidden by others. The dashed curves mark where the surface S^{∞} of saddle-node bifurcations at ∞, which is not part of the bifurcation set, would intersect.

As in the previous section, we distinguish local features which occur in a small neighborhood of $(r, \theta) = (0, 0)$ for the parameters near $b = 1,\ \varphi = 3\pi/2,\ \alpha = 0$, and global features which do not.

If α is sufficiently small, *both* secondary equilibria occur in a given characteristic neighborhood of $(r, \theta) = (0, 0)$. (This can be explained in the bifurcation set by the fact that for $\alpha = 0$ the surfaces $\pitchfork^{\infty}$ and S_1 intersect.) A limit cycle around the secondary equilibria remains entirely in the characteristic neighborhood from its birth in the Hopf bifurcation T_+ until it hits the saddle point and vanishes in the homoclinic connection $\dagger$.

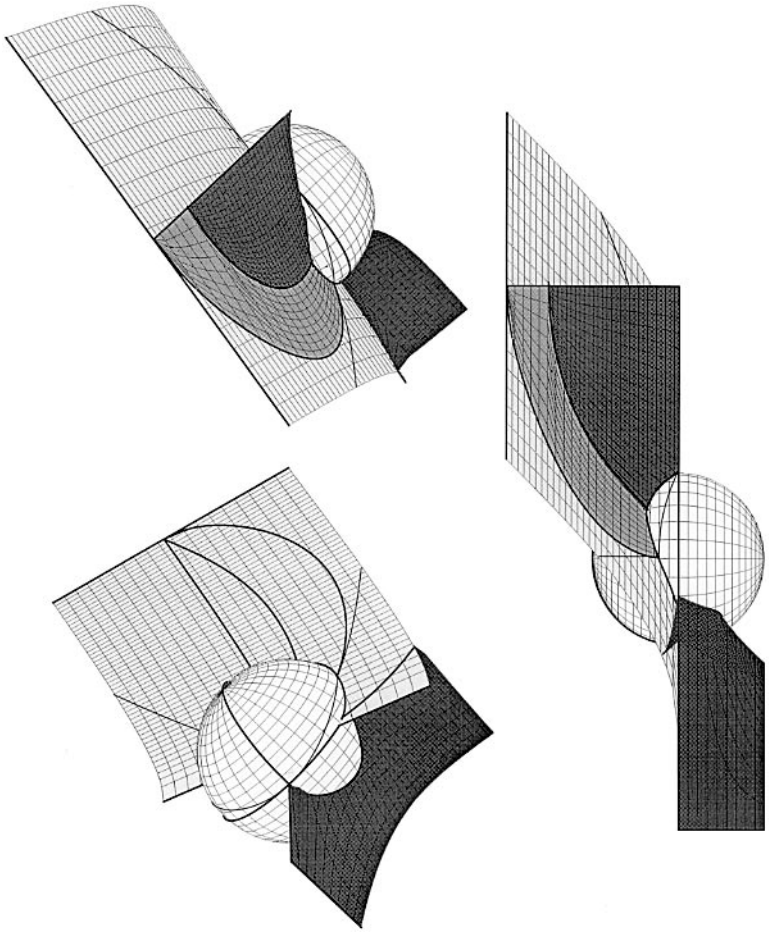

FIGURE 15. The surfaces of the bifurcation set intersecting a sphere around the organizing center $b = 1$, $\varphi = 3\pi/2$, $\alpha = 0$. To identify the viewpoints, compare Figure 14.

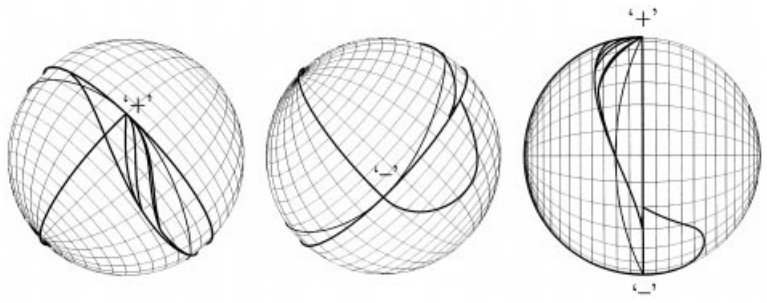

FIGURE 16. The curves of codimension-two bifurcations on the sphere around $b = 1$, $\varphi = 3\pi/2$, $\alpha = 0$, seen from the same viewpoints as in Figure 15.

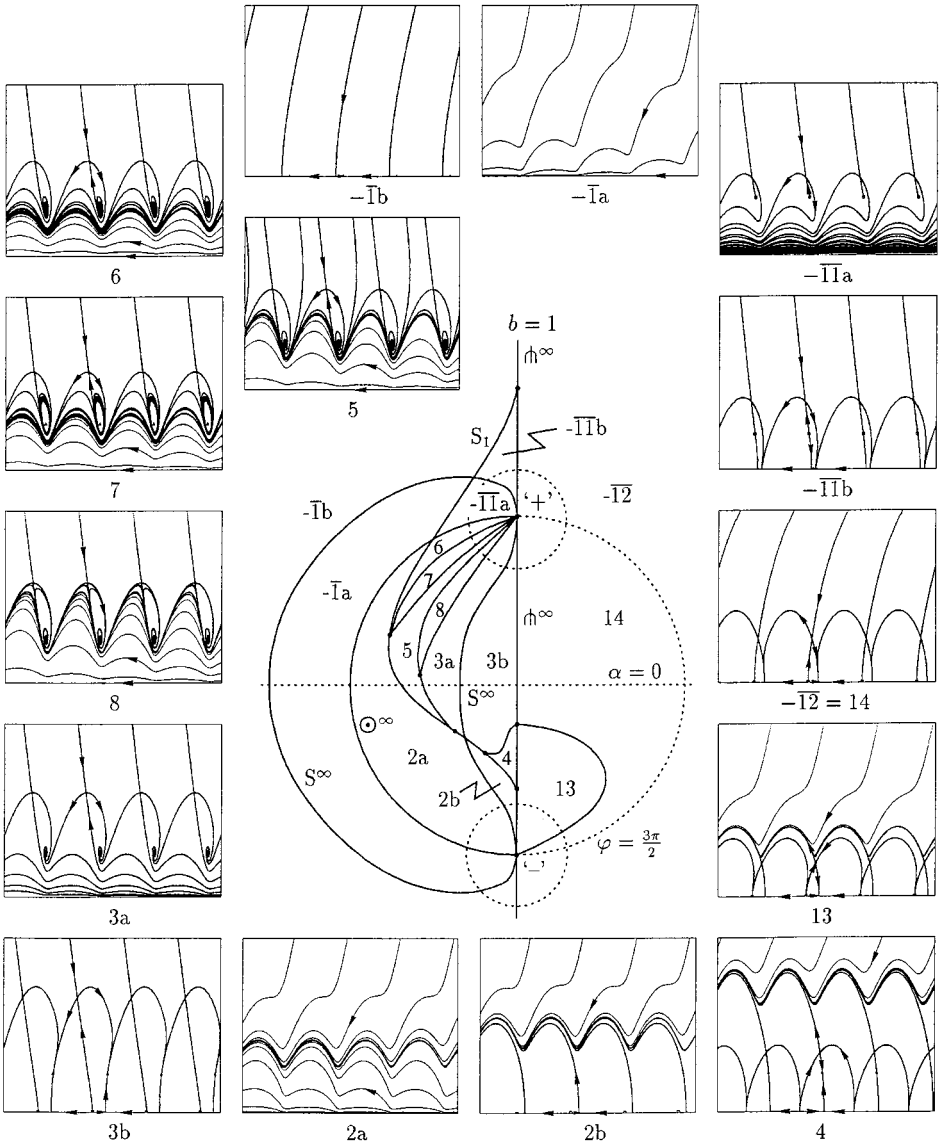

FIGURE 17. The regions of generic phase portraits of (3) on the sphere around $b = 1$, $\varphi = 3\pi/2$, $\alpha = 0$. The sketch in the middle shows the sphere of Figure 16 stereographically projected onto the (b, α)-plane.

We conclude that in this setting a phenomenon is local unless it is topologically global.

As the parameters approach the point $b = 1$, $\varphi = 3\pi/2$, $\alpha = 0$, all phase portraits converge to the one depicted in panel 0 of Figure 6. In particular, all topologically global phenomena, that is, limit cycles and heteroclinic connections, converge to the invariant circle $\{r = 0\}$. In other words, we can define a characteristic neigborhood U_c of the invariant circle such that we have the following. It is possible to find a neighborhood U_p in parameter space of the point $b = 1$, $\varphi = 3\pi/2$, $\alpha = 0$, such that it is sufficient to

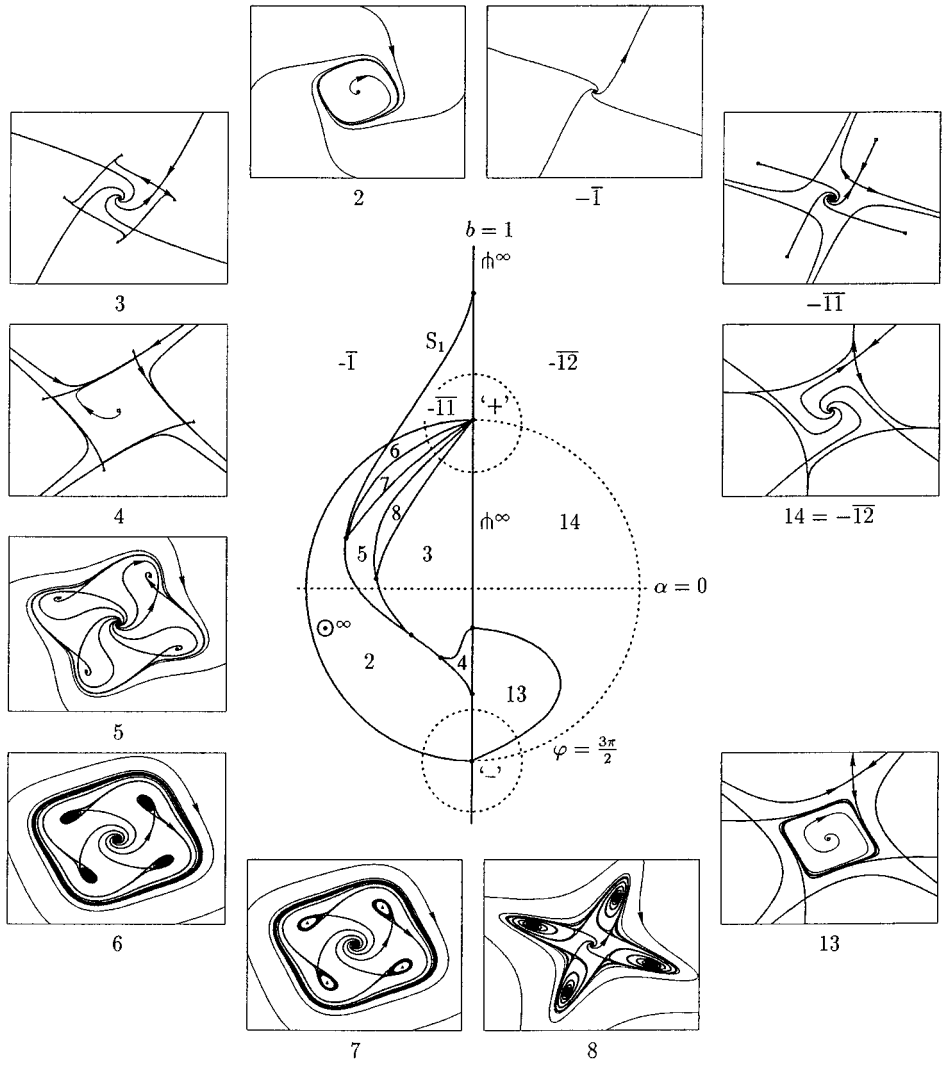

FIGURE 18. All generic phase portraits of (2) occur locally around $b = 1$, $\varphi = 3\pi/2$, $\alpha = 0$, if we take the symmetries $(z, t) \mapsto (\bar{z}, t)$ and $(z, t) \mapsto (\bar{z}, -t)$ into account and neglect saddle-node bifurcations at ∞. This is why we call this point an organizing center.

study (3) in $U_c \times U_p$. By this we mean that no topologically global phenomena, such as limit cycles and heteroclinic connections, intersect the boundary of U_c for $(b, \varphi, \alpha) \in U_p$.

Topologically global phenomena are discussed in the next section and we proceed by taking the local viewpoint, again neglecting the fact that (3) is defined on a half-cylinder. We want to show that (3) is a generic unfolding of the singularity giving the connection between case '$-$' and case '$+$', when the r^2 term in the equation for $\dot{\theta}$ vanishes. The problem is finding the unfolding of the corresponding singularity in the class of reflectionally equivariant planar vector fields. The codimension-three unfoldings

of the corresponding singularity in the class of reflectionally equivariant planar vector fields are studied in [**KR96**]. Here we present the general normal form and the unfoldings needed to discuss the special case at hand.

THEOREM 9. *In the class of reflectionally symmetric planar vector fields the normal form of the unfolding of a generic codimension-three singularity given by the vanishing of the r^2 term in (8) is*

$$\dot{r} = \mu_1 r - ar\theta - r^3 + O(|(r,\theta)|^5), \quad \dot{\theta} = \mu_2 + \mu_3 r^2 - \theta^2 + br^4 + O(|(r,\theta)|^5) \tag{10}$$

in a neighborhood of $(r, \theta, \mu_1, \mu_2, \mu_3) = (0, 0, 0, 0, 0)$.

The four-jet of this normal form is an unfolding in the parameters (μ_1, μ_2, μ_3) for fixed (a, b) satisfying the genericity conditions that $a \notin \{0, 1/2, 1\}$, $b \neq 0$, $a^2 b \neq 1$, $ab \neq 1$, $(2a-1)b \neq 1$, and that (a, b) is off a curve γ in the (a, b)-plane that does not have a parametrization but has been calculated numerically. The unfoldings are conjecturally versal for $a^2 b \leq 1$.

Near $(a, b) = (1/2, 0)$ the unfoldings are as shown in Figure 19 on a sphere around the central singularity as illustrated in Figure 20.

Sketch of the proof. The paper [**KR96**] is entirely dedicated to the proof of this theorem, and it is the source where more details and all unfoldings can be found. Consider the two-jet in normal form (compare (8)), with general reflectionally equivariant third- and fourth-order terms

$$\begin{aligned} \dot{r} &= -ar\theta + a_{30}r^3 + a_{12}r\theta^2 + a_{31}r^3\theta + a_{13}r\theta^3 + O(|(r,\theta)|^5) \\ \dot{\theta} &= \theta^2 + b_{21}r^2\theta + b_{03}\theta^3 + b_{40}r^4 + b_{22}r^2\theta^2 + b_{04}\theta^4 + O(|(r,\theta)|^5). \end{aligned}$$

By changing coordinates (compare [**GH86**]) to $(X, Y, T) = (x + Axy, y + Bx^2 + Cy^2, (1 + DY)^{-1}t)$ we can remove all third-order terms except for the r^3 term for a suitable choice of A, B, C, D, provided $a \neq 1$. The second coordinate change $(u, v) = (X + \tilde{A}X^3 + \tilde{B}XY^2, Y + \tilde{C}X^2Y + \tilde{D}Y^3)$ eliminates all fourth-order terms except for the X^4 term for a suitable choice of $\tilde{A}, \tilde{B}, \tilde{C}, \tilde{D}$, provided $a \neq 1/2$. The coefficient of the u^3 term can be chosen to be -1 if it is generic, that is, nonzero. Using the natural unfolding in (μ_1, μ_2, μ_3) the result follows.

Clearly, we need to study the four-jet

$$\dot{r} = \mu_1 r - ar\theta - r^3, \quad \dot{\theta} = \mu_2 + \mu_3 r^2 - \theta^2 + br^4 \tag{11}$$

in an effort to find all unfoldings. (Note that the genericity conditions $a \neq 0$ and $a \neq 1$ come from considering the codimension-two singularities; compare [**Ta74a**].)

We briefly discuss the singularity for $(\mu_1, \mu_2, \mu_3) = (0, 0, 0)$ by replacing it by a circle, so that each point on the circle corresponds to the direction of a parabola; for details see [**KR96**]. The chart $(r, \theta) = (\varepsilon, \varepsilon^2\Theta)$ in the direction of r gives, after division by ε^2,

$$\dot{\varepsilon} = -\varepsilon(a\Theta + 1), \quad \dot{\Theta} = b + 2\Theta + (2a-1)\Theta^2. \tag{12}$$

Studying this equation, one finds the appearance of two invariant parabolas for $(2a - 1)b = 1$ and a parabola of equilibria for $a^2 b = 1$. This shows that the genericity

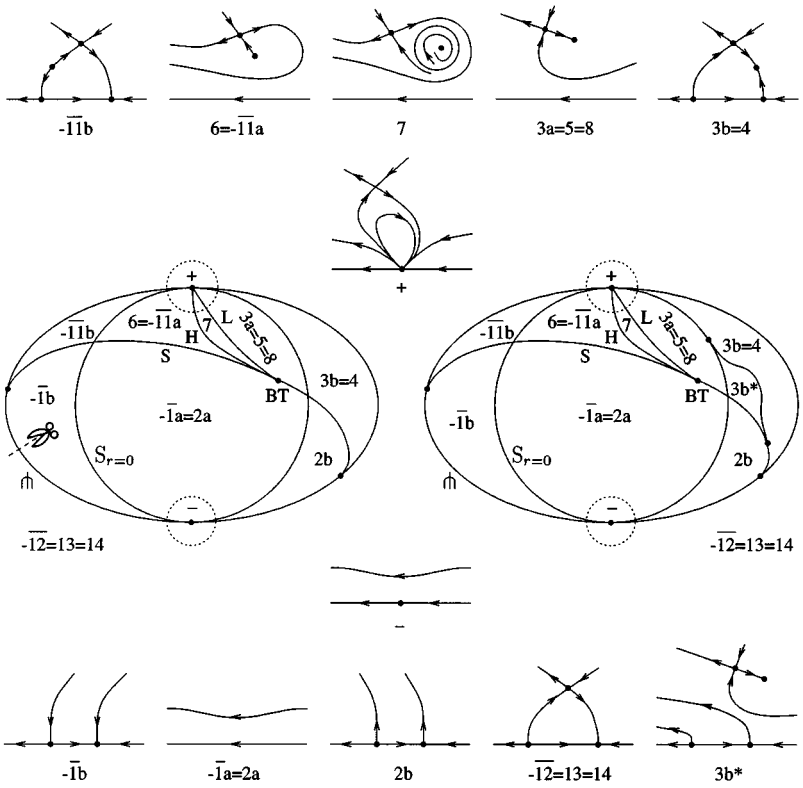

FIGURE 19. The unfolding near $(r, \theta, \mu_1, \mu_2, \mu_3) = (0, 0, 0, 0, 0)$ for $b \leq 0$ (left) and $b > 0$ (right) and $a \in (0, 1)$ as given by (10) on a sphere around $(\mu_1, \mu_2, \mu_3) = (0, 0, 0)$. The bifurcation diagram on the left is equivalent to Figure 17 from the local point of view, which can be see by cutting the circle ⋔ where indicated and pulling it straight.

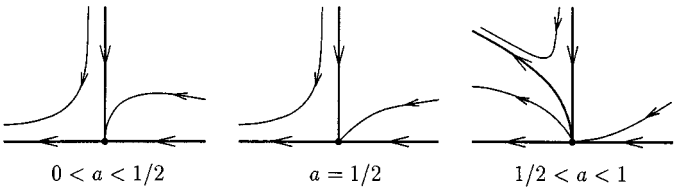

FIGURE 20. The central singularity of (10) for $a \in (0, 1)$.

conditions $a \neq 1/2$, $a^2 b \neq 1$ and $(2a-1)b \neq 1$ come from considering the codimension-three singularity.

We return to the question of finding the unfoldings, for which we need to study (11) and show that all phenomena are structurally stable. The following local bifurcations can be found by straightforward calculations.

- There is a surface $S_{r=0}$ of saddle-node bifurcations on the invariant line $\{r = 0\}$ given by $\mu_2 = 0$.
- There is a surface Λ of pitchfork bifurcations, given by $\mu_2 = (\mu_1/a)^2$.
- There is a surface S of saddle-node bifurcations off the invariant line, given by

$$\mu_2 = -\frac{4b\mu_1^2 + 4\mu_1\mu_3 + a^2\mu_3^2}{4(1-a^2b)}, \quad \text{where } \mu_1 \geq -a^2\mu_3/2, \text{ if } a^2b < 1$$

  and

$$\mu_1 \leq -a^2\mu_3/2, \quad \text{if } a^2b > 1.$$

- There is a surface H of Hopf bifurcation, given by

$$\mu_2 = \frac{(1-b)\mu_1^2 + (a-1)\mu_1\mu_3}{(a-1)^2},$$
$$\text{where } \mu_1(1-a) > 0 \text{ and } \mu_3 a - \frac{2\mu_1(1-ab)}{1-a} > 0.$$

- The intersection of S and H is a curve BT of Bogdanov–Takens points, given by

$$(\mu_2, \mu_3) = \left(\frac{(a-2+ab)\mu_1^2}{a(a-1)^2}, -\frac{2(1-ab)\mu_1}{a(a-1)}\right), \quad \text{where } \mu_1(1-a) > 0.$$

  The bifurcating Hopf bifurcation is supercritical (attracting limit cycle) for $\mu_1(a^2b-1) < 0$ and subcritical (repelling limit cycle) for $\mu_1(a^2b-1) > 0$.

These local bifurcations form the skeleton of the different unfoldings. They give the genericity conditions $a \neq 0$, $a \neq 1$, $a^2b \neq 1$ and $a - 2 + ab \neq 0$.

For studying nonlocal bifurcations and the phase portraits including saddle connections we realize that, by taking $v = r^2$, one can reduce (11) to the quadratic system

$$\dot{v} = 2\mu_1 v - 2av\theta - 2v^2, \quad \dot{\theta} = \mu_2 + \mu_3 v - \theta^2 + bv^2. \tag{13}$$

This makes it possible to use strong results from the theory of quadratic planar systems. Since the line $\{v = 0\}$ is invariant, Theorem A in [**Co89**] applies, which says that a planar vector field with an invariant line can have at most one limit cycle, which is hyperbolic. Furthermore, saddle connections can occur along invariant lines of (13), corresponding to invariant parabolas of (11). In fact the boundary curve $b = 0$ in the (a, b)-plane is characterized by a heteroclinic connection between two saddle-nodes along an invariant parabola, a codimension-three phenomenon.

To complete the study we have topological arguments and/or numerical evidence that the homoclinic connections (associated with the Bogdanov–Takens bifurcation) and other possible heteroclinic connections occur and bifurcate in a generic fashion; see [**KR96**]. This supports our conjecture that the unfoldings for $a^2b \leq 1$ are versal. (For $a^2b \geq 1$ the unfoldings contain centers and are consequently not versal.) □

THEOREM 10. *In a neighborhood of the singularity* $(r, \theta, b, \varphi, \alpha) = (0, 0, 1, 3\pi/2, 0)$ *the vector field (3) yields the special case of (10) where* $(a, b) = (1/2, 0)$.

Proof. We make use of the calculations in the proof of Theorem 8. Changing coordinates by $\tilde{r} = (\sqrt{2/\cos\alpha})r$ in (9), dropping the tilde and plugging in the Taylor series expansion

for $\tan\alpha$ gives

$$\begin{aligned}\dot r &= \mu_1 r - \tfrac{1}{2} r\theta - r^3 + O(\mu_1^3 r, \mu_2 r\theta, \mu_1^2 r\theta, |r,\theta|^4)\\ \dot\theta &= \mu_2 + 4(\alpha + \tfrac{1}{3}\alpha^3 + \cdots) r^2 - \theta^2 + O(\mu_1^4, \mu_2\theta^2, \mu_1^2\theta^2, \theta^4).\end{aligned}$$

(Recall that $\mu_1 = (\varphi - 3\pi/2)/2$ and $\mu_2 = 2(b-1) + 4\mu_1^2$.)

Setting $\mu_3 = 4\alpha$ yields

$$\begin{aligned}\dot r &= \mu_1 r - \tfrac{1}{2} r\theta - r^3 + O(\mu_1^3 r, \mu_2 r\theta, \mu_1^2 r\theta, |r,\theta|^4)\\ \dot\theta &= \mu_2 + \mu_3 r^2 - \theta^2 + O(\mu_1^4, \mu_2\theta^2, \mu_1^2\theta^2, \mu_3^3 r^2, \theta^4),\end{aligned} \tag{14}$$

which is a small perturbation of the special case of (10), where $a = 1/2$ and $b = 0$. This can be seen by blowing up this equation using

$$r = u\tilde r, \quad \theta = u^2\tilde\theta, \quad \mu_1 = u^2\tilde\mu_1, \quad \mu_2 = u^4\tilde\mu_2, \quad \mu_3 = u^2\tilde\mu_3, \quad \tau = u^2 t. \qquad \square$$

The unfolding for $(a, b) = (1/2, 0)$ is given by the bifurcation diagram in Figure 19 (left) on the sphere with the central singularity given by Figure 20 (middle). Comparing Figures 19 (left) and 17 shows that (14) indeed captures all behavior of (3) in a neighborhood of $(r, \theta) = (0, 0)$. (We have labeled the regions in Figure 19 with the numbers of the regions in Figure 17 to which they correspond.)

We finish with a discussion of the fact that the model (3) yields a singularity at infinity that is located at the intersection of the curves $a = 1/2$ and $b = 0$, which belong to the set of boundary curves in the (a, b)-plane. When we started this study we expected this singularity to be of codimension three since the values $a = 1/2$ and $b = 0$ play no role in the codimension-two unfoldings. Only after a detailed study of the singularity and of its unfoldings did we notice that this point is of higher codimension, possibly of codimension five.

The reason for a being exactly $1/2$ in (14) lies in the original $\mathbb{Z}_4$-equivariance. Since (2) is, in particular, $\mathbb{Z}_2$-equivariant (under the rotation by π), (3) is reflectionally symmetric. However, because (2) is even $\mathbb{Z}_4$-equivariant, the coefficient of the $r\theta$ term in (14) is forced to be the exceptional value $a = 1/2$, as can be seen from the calculations in the proof of Theorem 8. In other words, the fact that (2) is $\mathbb{Z}_4$-equivariant forces us to stay in the slice $a = 1/2$ of the (a, b)-plane of (11). (Crossing the line $a = 1/2$ changes the central singularity in Figure 20 from (left) to (right), but does not change the bifurcation diagram on the sphere.)

Since we started out with the truncated normal form (2), the blow-up at infinity given by (3) does not contain higher-order terms in r in the equation for $\dot\theta$. As a result we get the special case $b = 0$. Along the boundary curve $b = 0$ in the (a, b)-plane of (11) there is a heteroclinic connection along the invariant line $\{\theta = 0\}$ between two saddle-nodes. (Crossing the b-axis results in the change of the bifurcation diagram in Figure 19 from (left) to (right), namely an additional curve of saddle connections and the new phase portrait 3b* are born near one of the intersections of S and $S_{r=0}$.) Consequently, we should find a heteroclinic connection along an invariant line for any parameter value on the intersection curve SN^2 of the surfaces S_1 and S^∞. This is surprising, but easy to verify. From [**Kra94b**] or by a short calculation we know that the surface S_1 of the first

saddle-node bifurcation has the parametrization $\alpha = \varphi - \pi - \arcsin b$. By Theorem 3 the surface S^∞ of saddle-node bifurcation at ∞ is given by $b = |\sin\varphi|$. As a consequence, their intersection curve SN^2 has the parametrization $(b, \alpha) = (|\sin\varphi|, 0)$. However, if $\alpha = 0$ then the higher-order terms in (3) vanish along this curve. Furthermore, the line $\{\theta = 0\}$ is invariant since $b = |\sin\varphi|$.

We conclude that the curve SN^2 is of codimension three: along it there is a heteroclinic connection between a finite saddle-node and a saddle-node at infinity. So if we view (2) as a model on the Poincaré disc we must conclude that the curve SN^2 is not generic and could give rise to an additional surface of saddle connections near SN^2 and a new phase portrait on the Poincaré disc. (When considered on the cylinder this new bifurcation at infinity can be thought of as a change in the global topology of the unstable manifold of the saddle at infinity. Either this manifold goes directly to the attractor or it winds around the cylinder. In fact, it could wind an arbitrary number of times before reaching the attractor, giving rise to more topologically global bifurcations near SN^2.)

However, we mentioned earlier that a saddle-node bifurcation at infinity does not change the topological type of a phase portrait of (2) in the phase plane $\mathbb{C}$. This is why the surface S^∞ is not part of the bifurcation set in Figure 1. The curve SN^2 is only meaningful for the discussion of the compactification on the Poincaré disc. Consequently, it does not give rise to new surfaces that would be important for the original problem of finding all bifurcation sequences of (2).

We summarize this discussion by concluding that the local unfolding near the organizing center $b = 1$, $\varphi = 3\pi/2$, $\alpha = 0$, is in accordance with the conjectured nature of the bifurcation set of (2). By this we mean that no previously unknown surfaces have been found that would give rise to new bifurcation sequences. We see this as evidence for our conjecture that the bifurcation set is as depicted in Figure 1.

10. *Topologically global phenomena*

It is the ultimate goal to also show that the topologically global phenomena unfold versally in (3). The main difficulty is to connect the local information from the last section with our information on topologically global phenomena. Given a saddle point in the characteristic neighborhood, the question is whether it can give rise to, for example, a topologically global homoclinic connection. To this end one needs to define a return map from the boundary of a suitable neighborhood of $(r, \theta) = (0, 0)$ to itself, and combine it with the local information in this neighborhood. The present case is similar to the problem of unfolding a cuspidal loop and it seems plausible that the technique of *desingularizing a family of vector fields* as presented in [**Du93**, **Rou93a**, **Rou93b**, **Pan97**] can also be used in our case. This line of thought is under investigation and beyond the scope of this paper.

If there is a saddle point in the characteristic neighborhood of the singularity, let d_- (respectively d_+) be the value of r of the first intersection of its unstable (respectively stable) manifold with the line $\{\theta = -\pi\}$. The problem is to find an analytic expression, or at least an asymptotic expansion, of the surface given by $d_- = d_+$; compare Figure 21. To this end one has to calculate the zeros of certain Mel'nikov-like integrals depending on parameters; this is not done here. Note, however, that we have computed the surface

$\{d_- = d_+\}$ for the cases $\square_1$ and $\boxtimes$ numerically by continuation with AUTO.

We conclude with some observations concerning the question as to how the surfaces $\curlywedge$, $\square_1$, $\boxtimes$ and $\circledcirc$ tend to the line $b = 1$, $\varphi = 3\pi/2$. Apart from numerical evidence, the motivation is the following lemma.

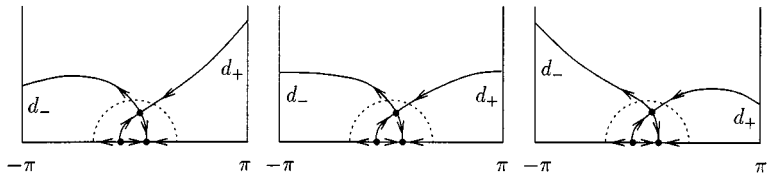

FIGURE 21. Topologically global phenomena cannot be detected inside a characteristic neighborhood around the singularity $(r, \theta) = (0, 0)$. Note that the curve $\{d_- = d_+\}$ is followed in parameter space when one computes a saddle connection numerically by continuation.

LEMMA 11. *For fixed $\alpha \in (0, \pi)$ the curve T_+ of secondary Hopf bifurcations converges to $b = 1$, $\varphi = 3\pi/2$, under an angle $\Theta(\alpha)$ with the line $\varphi = 3\pi/2$, $b \leq 1$, for which we have the following:*

- *$\Theta(\alpha)$ is positive for $\alpha \in (0, \pi/2)$, zero for the Hamiltonian case $\alpha = \pi/2$ and negative for $\alpha \in (\pi/2, \pi)$;*
- *$\Theta(\alpha)$ converges to $\pi/2$ as $\alpha \to 0$ and to $-\pi/2$ as $\alpha \to \pi$;*
- *$\Theta(\alpha)$ is a strictly monotonic function on $(0, \pi)$.*

Proof. Consider the case $\alpha \in (0, \pi/2]$, so that the surface T_+ is in the cube of interest. For points on T_+ we have, see [**Kra94b**],

$$2 \tan\alpha \cos\varphi = \sin\varphi - \sqrt{b^2 - \cos^2\varphi}.$$

Calculating b as a function of φ gives

$$b(\varphi) = \sqrt{1 - 4\tan\alpha \sin\varphi \cos\varphi + 4\tan^2\alpha \cos^2\varphi},$$

and

$$b'(\varphi) = -\frac{8\tan^2 \sin\varphi \cos\varphi + 4\tan\alpha(\cos^2\varphi - \sin^2\varphi)}{2\sqrt{1 - 4\tan\alpha \sin\varphi \cos\varphi + 4\tan^2\alpha \cos^2\varphi}}.$$

Consequently, one gets $\tan(\pi/2 + \Theta(\alpha)) = b'(3\pi/2) = 2\tan\alpha$. In complete analogy one calculates $\Theta(\alpha)$ for $\alpha \in [\pi/2, \pi)$, which yields

$$\Theta(\alpha) = \begin{cases} \arctan(2\tan\alpha) - \pi/2 & \text{if } \alpha \in (0, \pi/2) \\ 0 & \text{if } \alpha = \pi/2 \\ \arctan(2\tan\alpha) + \pi/2 & \text{if } \alpha \in (\pi/2, \pi). \end{cases}$$

It is now easily checked that $\Theta(\alpha)$ has the mentioned properties. □

We have computed cross-sections of the surfaces $\curlywedge$, $\square_1$, $\boxtimes$ and $\circledcirc$ near the point $b = 1$, $\varphi = 3\pi/2$ for various fixed values of α. The calculations become more difficult as this point is approached and break down before it is reached. This makes it quite difficult to make statements about orders of contact. Nevertheless, our observation is that the surfaces approach the point in angles; compare Figure 7.

CONJECTURE 12. (Based on numerical results) *For $\alpha \in (0, \pi)$ the curves $\curlywedge$, $\boxtimes$ and $\circledcirc$ converge to $b = 1,\ \varphi = 3\pi/2$ under an angle $\Lambda(\alpha)$ with the line $\varphi = 3\pi/2,\ b \leq 1$. The angle $\Lambda(\alpha)$ has the same properties as $\Theta(\alpha)$ from Lemma 11.*

For $\alpha \in (-\pi, 0)$ the curve $\square_1$ converges to $b = 1,\ \varphi = 3\pi/2$, under an angle $\Delta(\alpha)$ with the line $\varphi = 3\pi/2,\ b \geq 1$, for which we have the following:

- *$\Delta(\alpha)$ is positive for $\alpha \in (-\pi, -\pi/2)$, zero for the Hamiltonian case $\alpha = -\pi/2$ and negative for $\alpha \in (-\pi/2, 0)$;*
- *$\Delta(\alpha)$ converges to $\pi/2$ as $\alpha \to -\pi$ and to $-\pi/2$ as $\alpha \to 0$;*
- *$\Delta(\alpha)$ is a strictly monotonic function on $(-\pi, 0)$.*

Acknowledgements. For stimulating discussions and encouragement I thank V. I. Arnol'd, R. I. Bogdanov, H. W. Broer, E. Doedel, F. Dumortier, S. van Gils, J. Guckenheimer, Yu. S. Il'yashenko, A. I. Khibnik, M. Krupa, Yu. A. Kuznetsov, A. I. Neishtadt, E. V. Nikolaev, C. Rousseau and F. Takens.

A travel grant from the Nederlands Organization for Scientific Research (NWO), and the support and hospitality of the Centre de Recherches Mathématiques, Montréal, the Center for Applied Mathematics, Ithaca, and the Russian Academy of Sciences are gratefully acknowledged.

REFERENCES

[Arn77] V. I. Arnol'd. Loss of stability of self-oscillation close to resonance and versal deformations of equivariant vector fields. *Functional Anal. Appl.* **11** (1977), 85–92.

[Arn78] V. I. Arnol'd. *Geometrical Methods in the Theory of Ordinary Differential Equations*, 2nd edn. Springer, Berlin, 1988. (Transl. from V. I. Arnol'd. *Supplemantary Chapters in the Theory of Ordinary Differential Equations*. Nauka, Moscow, 1978.)

[AAIS86] V. I. Arnol'd, V. S. Afrajmovich, Yu. S. Il'yashenko and L. P. Shil'nikov. I. Bifurcation theory. *Dynamical Systems V: Bifurcation Theory and Catastrophe Theory (Encyclopedia of Mathematical Sciences 5*). Ed. V. I. Arnol'd. Springer, Berlin, 1994. (Transl. from *Dinamicheskie Sistemy 5*. VINITI, Moscow, 1986.)

[BGMWW92] A. Back, J. Guckenheimer, M. R. Myers, F. J. Wicklin and P. A. Worfolk. DsTool: Computer assisted exploration of dynamical systems. *Notices Amer. Math. Soc.* **39** (1992), 303–309.

[BK79] F. S. Berezovskaya and A. I. Khibnik. On the problem of bifurcations of self-oscillations close to a 1:4 resonance. *Sel. Math. Form. Sov.* **13** (1994), 197–215. (Transl. from On the problem of auto-oscillation bifurcations near 1:4 resonance (investigation of the model equation). *Preprint*, Research Computing Center Acad. Sci. USSR, Pushchino, 1979 (in Russian).)

[BK80] F. S. Berezovskaya and A. I. Khibnik. On the bifurcations of separatrices in the problem of stability loss of auto-oscillations near 1:4 resonance. *Prikl. Math. Mech.* **44** (1980), 663–667.

[BR93] T. R. Blows and C. Rousseau. Bifurcation at infinity in polynomial vector fields. *J. Diff. Eq.* **104** (1993), 215–242.

[Bog76a] R. I. Bogdanov. Bifurcations of a family of vector fields on the plane. *Tr. Semin. Im. I. G. Petroskogo* **2** (1976), 23–36. (Transl. in *Sel. Math. Sov.* **1** (1981), 373–387.)

[Bog76b] R. I. Bogdanov. Versal deformation of a singularity of a vector field on the plane in case of zero eigenvalues. *Tr. Semin. Im. I. G. Petroskogo* **2** (1976), 37–65. (Transl. in *Sel. Math. Sov.* **1** (1981), 389–421.)

[Ca81] J. Carr. *Applications of Centre Manifold Theory (Applied Mathematical Science 35)*. Springer, New York, 1981.

[CLW94] S.-N. Chow, C. Li and D. Wang. *Normal Forms and Bifurcation of Planar Vector Fields*. Cambridge University Press, 1994.

[Co89] W. A. Coppel. Some quadratic systems with at most one limit cycle. *Dynamics Reported*, vol. 2. Eds U. Kirchgraber and H. O. Walther. Wiley, 1989, pp. 61–88.

[Doe86] E. Doedel. Auto: Software for continuation and bifurcation problems in ordinary differential equations. California Institute of Technology, Pasadena, California, 1986.

[Du93] F. Dumortier. Techniques in the theory of local bifurcations: blow-up, normal form, nilpotent bifurcations, singular perturbations. *Bifurcations and Periodic Orbits of Vector Fields.* Ed. D. Schlomiuk. NATO ASI Series C **408** (1993), 19–73.

[DR93] F. Dumortier and R. Roussarie. Tracking limit cycles escaping from rescaling domains. *Proc. Int. Conf. Dynamical Systems and Related Topics (Adv Ser. Dyn. Syst. 9).* Word Scientific, 1991, pp. 80-99.

[DRSZ91] F. Dumortier, R. Roussarie, J. Sotomayor and H. Żołądek. *Bifurcations of Planar Vector Fields: Nilpotent Singularities and Abelian Integrals (Lecture Notes in Mathematics 1480)*. Springer, 1991.

[GH86] J. Guckenheimer and P. Holmes. *Nonlinear Oscillations, Dynamical Systems, and Bifurcations of Vector Fields*, 2nd printing. Springer, 1986.

[Kho79] E. I. Khorosov. Versal deformations of equivariant vector fields for the case of symmetries of orders 2 and 3. *Tr. Semin. Im. I. G. Petrovskogo* **5** (1979), 163–192. (Transl. in *Topics in Modern Mathematics (Petrovskij Seminar 5)* (1985), 207–243.)

[Kra94a] B. Krauskopf. Bifurcation sequences at 1:4 resonance: an inventory. *Nonlinearity* **7** (1994), 1073–1091.

[Kra94b] B. Krauskopf. The bifurcation set for the 1:4 resonance problem. *Experimental Mathematics* **3** (1994), 107–128.

[Kra95] B. Krauskopf. On the 1:4 Resonance problem: analysis of the bifurcation set. *Doctoral Thesis*, University of Groningen, May 1994.

[KR96] B. Krauskopf and C. Rousseau. Codimension-three unfoldings of reflectionally symmetric vector fields. *Preprint*, Centre de Recherches Mathématiques, CRM-2365 (available via http://www.crm.umontreal.ca). Submitted to *Nonlinearity*.

[Nei78] A. I. Neishtadt. Bifurcations of the phase patterns of an equation system arising in the problem of stability loss of self-oscillation close to 1:4 resonance. *Prikl. Math. Mech.* **42** (1978), 896–907.

[Pan97] D. Panazzolo. Desingularization of nilpotent singularities in analytic families. *PhD Thesis*, Université de Bourgogne, 1997.

[Rou93a] R. Roussarie. Desingularization of unfoldings of cuspidal loops. *Geometry and Analysis in Nonlinear Dynamics (Pitman Res. Notes Math. Series, 222)*. Eds H. W. Broer and F. Takens. Longman, 1992, pp. 41–55.

[Rou93b] R. Roussarie. Techniques in the theory of local bifurcations: cyclicity and desingularization. *Bifurcations and Periodic Orbits of Vector Fields*. Ed. D. Schlomiuk. NATO ASI Series C **408** (1993), 347–382.

[Ta74a] F. Takens. Singularities of vector fields. *Publ. Math. IHES* **43** (1974), 47–100.

[Ta74b] F. Takens. Forced oscillations and bifurcations. *Applications of Global Analysis I (Communications of the Mathematical Institute 3).* Rijksuniversiteit, Utrecht, 1974.

[Wo88] S. Wolfram. *Mathematica, A System for Doing Mathematics by Computer*. Addison-Wesley, 1988.